Research and Development Technical Report

ECOM-76-1301-7

REPETITIVE SERIES INTERRUPTER II

Robert F. Caristi
Robert P. Simon
David V. Turnquist
EG&G INC.
35 Congress Street
Salem, MA. 01970

June 1978

Seventh Interim Report for the Period 1 October 1977 to 31 January 1978

Prepared for:

ECOM

US ARMY ELECTRONICS COMMAND FORT MONMOUTH, NEW JERSEY 07703

DISCLAIMER NOTICE

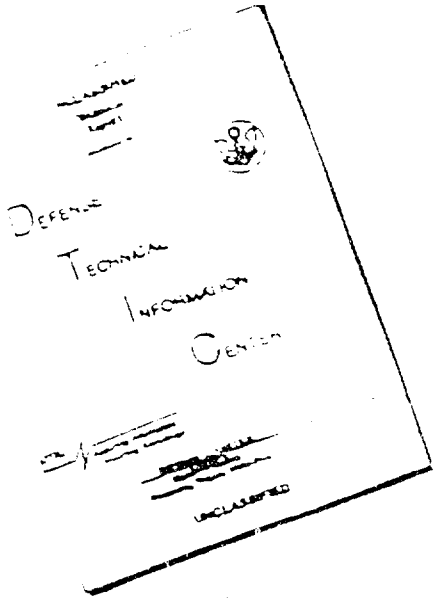

THIS DOCUMENT IS BEST QUALITY AVAILABLE. THE COPY FURNISHED TO DTIC CONTAINED A SIGNIFICANT NUMBER OF PAGES WHICH DO NOT REPRODUCE LEGIBLY.

NOTICES

Disclaimers

The findings in this report are not to be construed as an official Department of the Army position, unless so designated by other authorized documents.

The citation of trade names and names of manufacturers in this report is not to be construed as official Government indorsement or approval of commercial products or services referenced herein.

Disposition

Destroy this report when it is no longer needed. Do not return it to the originator.

Interim rept. no. 7, 1 Oct 77-31 Jan 78,

UNCLASSIFIED

SECURITY CLASSIFICATION OF THIS PAGE (When Data Entered)

REPORT DOCUMENTATION PAGE	READ INSTRUCTIONS BEFORE COMPLETING FORM
1. REPORT NUMBER: ECOM-76-1301-7 ✓	2. GOVT ACCESSION NO. / 3. RECIPIENT'S CATALOG NUMBER
4. TITLE (and Subtitle): REPETITIVE SERIES INTERRUPTER II	5. TYPE OF REPORT & PERIOD COVERED: Seventh Interim Report ✓ 1 Oct 77 to 31 Jan 78
	6. PERFORMING ORG. REPORT NUMBER
7. AUTHOR(s): Robert F. Caristi, Robert P. Simon, David V. Turnquist	8. CONTRACT OR GRANT NUMBER(s): DAAB07-76-C-1301 ✓
9. PERFORMING ORGANIZATION NAME AND ADDRESS: EG&G Inc., Electronic Components Div. ✓ 35 Congress Street Salem, Massachusetts 01970	10. PROGRAM ELEMENT, PROJECT, TASK AREA & WORK UNIT NUMBERS: 612705 1L1 62705.AH.94.E1.08
11. CONTROLLING OFFICE NAME AND ADDRESS: US Army Electronics Technology and Devices Lab. ATTN: DELET-BG Fort Monmouth, NJ 07703	12. REPORT DATE: June 1978 / 13. NUMBER OF PAGES: 61
14. MONITORING AGENCY NAME & ADDRESS (if different from Controlling Office)	15. SECURITY CLASS. (of this report): Unclassified / 15a. DECLASSIFICATION/DOWNGRADING SCHEDULE

16. DISTRIBUTION STATEMENT (of this Report)

Approved for Public Release; Distribution Unlimited

17. DISTRIBUTION STATEMENT (of the abstract entered in Block 20, if different from Report)

DDC REPRODUCED JUL 5 1978 F

18. SUPPLEMENTARY NOTES

19. KEY WORDS (Continue on reverse side if necessary and identify by block number)

Series Interrupter
Gas Filled Device
Fuse
Thyratron
Magnetic Interaction Region

20. ABSTRACT (Continue on reverse side if necessary and identify by block number)

The interruption characteristics have been established for six developmental "plasma chute" interrupters, five rated at 15 kV and one rated at 30 kV. Six-hundred ampere interruptions at 20 kV have been achieved with a magnetic field energy of less than 8 joules. The most efficient interaction channel geometry has been found to be one which contains both a "chuted" surface against which the discharge is magnetically driven, and an unchuted (smooth) surface located behind the driven discharge, the presence of which latter surface minimizes

DD FORM 1 JAN 73 1473 EDITION OF 1 NOV 65 IS OBSOLETE

UNCLASSIFIED

SECURITY CLASSIFICATION OF THIS PAGE (When Data Entered)

the availability of plasma to sustain the discharge. Typical interaction column drops have been found to be 300 to 400 volts per section (20 to 26 volts/cm) at reasonable tube pressures with no more than three (and possibly two) sections being adequate for the operation of tubes rated at 50 kV. Holdoff-section voltage drops of about 120 volts have been observed for holdoff sections capable of withstanding 30 kV. A total tube drop of 830 volts has been observed at the 25 kV, 18.5 A level. Linear extrapolation of existing data to the 50 kV, 1000 A level shows that reliable interruption should be achievable with a magnetic field energy of the order of 10 joules for an interrupter having a total tube drop of about 1200 volts, or 2.4% of the system's operating voltage.

ABBREVIATIONS AND SYMBOLS

A	Ampere(s)
Bq	Magnetic field required to reduce fault current to zero with a 50% probability
Crc	Capacitance of fault network
Cm	Capacitance of magnet circuit
d	Arbitrary unit of length
D	Diode in tube drop measuring circuit
Dch	Holdoff diode
eag	Peak anode to grid voltage
eb	Instantaneous anode voltage
Ebb	DC anode supply voltage
Ecc	Bias voltage
ecd	Voltage drop of interaction column (steady-state)
Ef	Cathode heater voltage
egk	Peak forward grid to cathode voltage
Em	DC supply voltage of magnet circuit
eo	Output voltage of tube drop measuring circuit
epy	Peak forward anode voltage
etd	Total voltage drop of conducting tube (steady-state tube drop)
Eres	Reservoir heater voltage
Hz	Hertz
ib	Peak forward anode current
im	Peak current through magnet coil
kV	Kilovolt(s)
kG	Kilogauss(es)
l	Active length of interaction column (per section)
Lch	Charging inductor
N	Number of turns in magnet coil
P	Gas pressure within tube
PFN	Pulse forming network

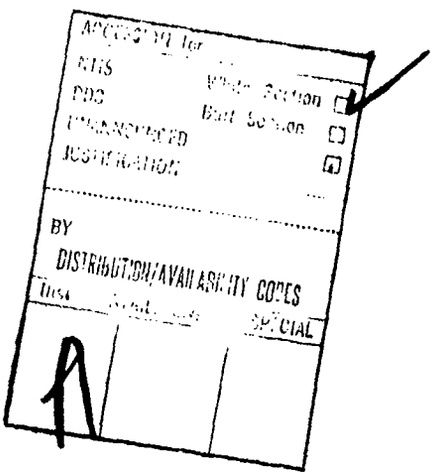

Rch	Charging resistor
Rl	Load resistance of pulse forming network
Rm	Magnet circuit damping resistance
Rrc	Load resistance of fault network
RSI	Repetitive series interrupter
t	Time
tp	Pulse width of pulse forming network
tr	Rise time of current in magnet circuit
TUT	Tube under test
V	Volts
Zn	Characteristic impedance of pulse forming network
Ω	Ohm(s)

TABLE OF CONTENTS

LIST OF ILLUSTRATIONS

LIST OF TABLES

1.0 FOREWORD

This Seventh Interim Technical Report presents the results of the first four months of a program of research and development conducted under Part II of ERADCOM Contract DAAB07-76-C-1301 entitled "Repetitive Series Interrupter II." It thus covers the period 1 October 1977 through 31 January 1978. In addition, experimental results are included which were obtained through 17 March 1978. These recent results are included to ensure that this report adequately reflects the current status and overall direction of the program. The work described herein was performed by EG&G, Inc., Electronic Components Division, 35 Congress Street, Salem, Massachusetts 01970.

2.0 INTRODUCTION AND SUMMARY

a. Purpose of the RSI Program

The purpose of Part II of the Repetitive Series Interrupter II Program is to develop a gas discharge device which functions as both a repetitively closable and openable switch at the 50 kV, 1000 A power level. In addition to twelve months of research and development work, the Program also entails the actual construction of five exploratory development RSI's designed to operate under the electrical conditions given in Table 1.

A repetitively closable and openable switch is clearly useful as an automatically resettable fuse. When used in series with a component to be protected (e.g., a traveling wave tube), the RSI can be made to function as an automatically openable switch in the event of a fault within the protected device. Upon the termination of fault conditions, the RSI can be made to function as an automatically closable switch so that normal system operation can be resumed.

Three mandatory characteristics of a practical RSI are thus implied: 1) the device must operate with a reasonable steady-state drop when in the conducting state; 2) the device must remain in the nonconducting state for a suitable period after receiving the command to switch off, i.e., the device must not restrike; and 3) the device must be either a) free-wheeling, i.e., automatically returnable to the conducting state, or b) retriggerable, i.e., returnable to the conducting state upon the application of a suitable triggering command.

The work described herein is directed toward the development of an RSI based primarily on hydrogen thyratron technology and construction techniques. Such an RSI may be closed by the application of a grid pulse as is a standard thyratron, maintained in the normally closed state by the use of a "keep-alive" current, and opened by the application of a pulsed magnetic field which is applied across an interaction channel built into the tube. An additional requirement is thus implied for a practical RSI device of this type, namely that the current within the RSI be extinguishable with a minimum of magnetic field energy.

Table 1. Desired Electrical Characteristics, Repetitive Series Interrupter (As Amended for Part II).

(a)	Open Circuit Holdoff Voltage	50 kV, Minimum
(b)	Normally Closed Voltage Drop	500 V, Maximum
(c)	Peak Fault Current	1000 A, Maximum
(d)	Normal Average Current	0.7 A, Minimum
(e)	Normal Peak Current	17 A, Maximum
(f)	Repetition Rate	1 kHz to 20 kHz (Burst Mode)
(g)	Life	1000 Hours, Minimum
(h)	Operating Mode	Normally Closed
(i)	Opening Actions	20,000 Cycles, Minimum

The principal goals of the RSI R&D Program are thus to develop an RSI which:

1. operates at 50 kV, 1000 A;
2. operates with a reasonably low steady-state tube drop;
3. does not restrike;
4. requires a minimum of interrupting magnetic field energy;
5. is of a design which lends itself to construction using established techniques and conventional materials;
6. is capable of providing a reasonable service life under the applicable operating conditions.

The ultimate purpose of the work described herein is to obtain the information necessary to construct five exploratory development RSI's most likely to operate under the conditions given in Table 1.

b. Current Status of the Program

Recent work has been directed toward the establishment of design criteria for the final series of RSI's which are to be built under the Program. The principal vehicles for this work have been the RSI 10 series of tubes which were built under Part I of the Program and which have proven to be efficient and reliable interrupters at the 15 to 30 kV, 300 A power level.

Section 3.0 presents the results of extensive tests which have been conducted to determine the performance of each member of the RSI 10 series. Six-hundred-ampere interruptions at 20 kV have already been achieved with a magnetic field energy of less than 8 joules. Parametric studies have been conducted which have established the magnetic fields required to extinguish high voltage, high current discharges for each tube design. The most efficient interaction channel geometry has been found to be one which contains a "chuted" surface against which the discharge is magnetically driven, and an unchuted (smooth) surface behind the discharge, the presence of which minimizes the availability of plasma to sustain the discharge. It has also been found that multiple, series interaction sections serve not only to extend the voltage capability of an RSI, but also improve the efficiency of the device.

Tests of both RSI's and standard production thyratrons have revealed that reasonable steady-state tube drops are achievable in efficient and practical interrupters, and a total RSI tube drop of 830 volts (corresponding to an interaction column field of 23 volts/cm) has been achieved at the 25 kV, 18.5 A level (etd = 0.033 epy).

The discussion of Section 3.0 also reflects briefly on certain observations relative to the restrike phenomenon, and it is concluded that a significant fraction (if not all) of the previously reported restrike incidence may in fact be retriggering and thus not true restriking of the discharge.

c. Conclusions and Plan for Future Work

The RSI 10 series proved to be an efficient and reliable family of RSI's which operated successfully at their design voltages and which firmly established the validity of the "plasma chuting" concept as a mechanism for reducing magnetic field requirements without introducing excessively high tube drops.

Section 4.0 reports the important conclusions to be reached from the experimental results to date, and presents the overall plan for future work. The design of the RSI 12 series is discussed (the final generation of RSI's under the Program) as well as plans for the elimination of restrike and the establishment of triggering characteristics and service life.

The overall conclusion is that the prognosis for the development of a successful Repetitive Series Interrupter is good. Linear extrapolation of existing data to the 50 kV, 1000 A level indicates that reliable interruption should be achievable with a magnetic field conservatively estimated to be less than 10 kG and with a total tube drop of about 1200 volts, or 2.4% of the system's operating voltage.

3.0 CHARACTERIZATION OF THE RSI 10 SERIES

a. Objectives

The RSI 10 series was designed and constructed as a result of the discovery that "plasma chutes" built into the walls of the interaction channel materially reduced the magnetic field required to interrupt a given discharge current at a given level of epy.[1,2] A total of six experimental tubes were built during Part I of the RSI program,[3,4] and the characterization of these tubes was the basis for the bulk of the work performed during this reporting period. The object of this investigation was not to characterize each member of the RSI 10 family in depth, but rather to observe overall trends. Thus insight could be gained into the mechanisms controlling the operation of chuted tubes, and a direction could be established for the design of a family of 50 kV tubes which would be most likely to operate satisfactorily under the conditions set forth in Table 1. It is not the object of this writing to show all of the data that were generated from the testing of the RSI 10 series, but rather to present a clear picture of the relative performances of these tubes to illustrate the trends which became evident during the course of the investigation. With this thought in mind, representative data for each tube are given in this section along with the results of the more important parametric studies.

b. Interaction Channel Geometry

The geometry of the interaction region of the RSI 10 series is shown in Figure 1. All interaction channels were made of ceramic (95% alumina), machined in the "green" state, and then subjected to high-temperature curing. Types A, B, and C had in common a bore diameter of 0.300 inch. Type A had both long (0.500 inch) and short (0.250 inch) chutes; Type B had 0.750 chutes on one side of the bore and none on the other; and Type C was similar to Type A except that the total number of chutes in the Type C was one-half that of Type A. Types D and E were similar to types A and B, respectively, except that the bores of the former tubes were 0.150 inch as opposed to 0.300 inch. Type DD was similar to Type D except that its total length was twice that of Type D (12 inches as opposed to 6 inches for Type D and also 6 inches for

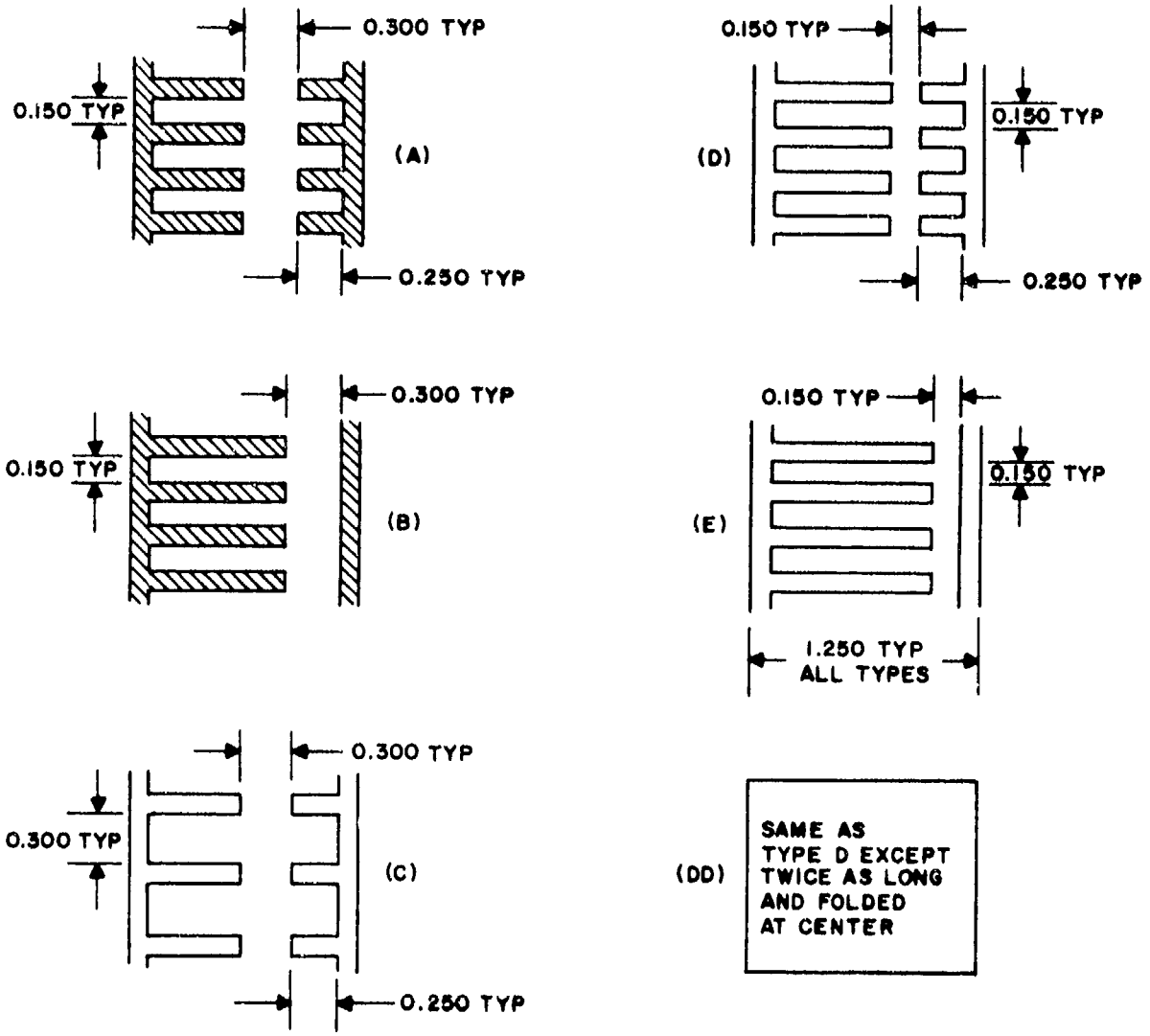

Figure 1. Schematic Representation of Interaction Channel Geometry (RSI 10 Series).

Types A, B, C, and E). All tubes except DD were equipped with a standard thyratron holdoff section (EG&G Type HY-6). RSI 10DD was equipped with a holdoff section specifically designed to minimize its steady-state drop. (Refer to RSI 11B, discussed in part e of this section.)

When testing a tube such as Type A, and by reversing the direction of the IXB force in the channel, one could drive the discharge into either the long or the short chutes as desired. With Type B, one could drive the discharge into the chutes in the presence of the wall, or into the wall in the presence of the chutes. Type C provided some insight as to the effects of varying the number of chutes when compared with Type A. Types D and E provided information regarding the effects of bore diameter when compared with Types A and B. Type DD (the double-length tube) was specifically designed to operate reliably at higher voltage levels.

c. Experimental Apparatus and Technique

(1) Determination of Magnetic Field Required for Interruption

The circuit of Figure 2 was used to determine the magnetic field required for current interruption. The TUT was triggered directly and its holdoff section was actively employed as opposed to relying on a series thyratron to provide holdoff capability. In this way, restrike activity could be observed simultaneously with magnetic field requirements.

The DC anode voltage of the TUT, Ebb, could be varied at will, as could the TUT hydrogen pressure, P. The fault circuit load resistor, Rrc, and the magnet circuit damping resistor, Rm, could be adjusted as desired. Rm was generally set to provide a somewhat underdamped current waveform in the magnet circuit, thus eventually establishing a negative voltage at the anode of the 1802 thyratron to ensure its recovery.

The number of turns, N, of the magnet coil was adjustable to permit alteration of the magnetic field risetime, tr, and the connections to the coil were reversible to permit changing the direction of the IXB force in the RSI's interaction region.

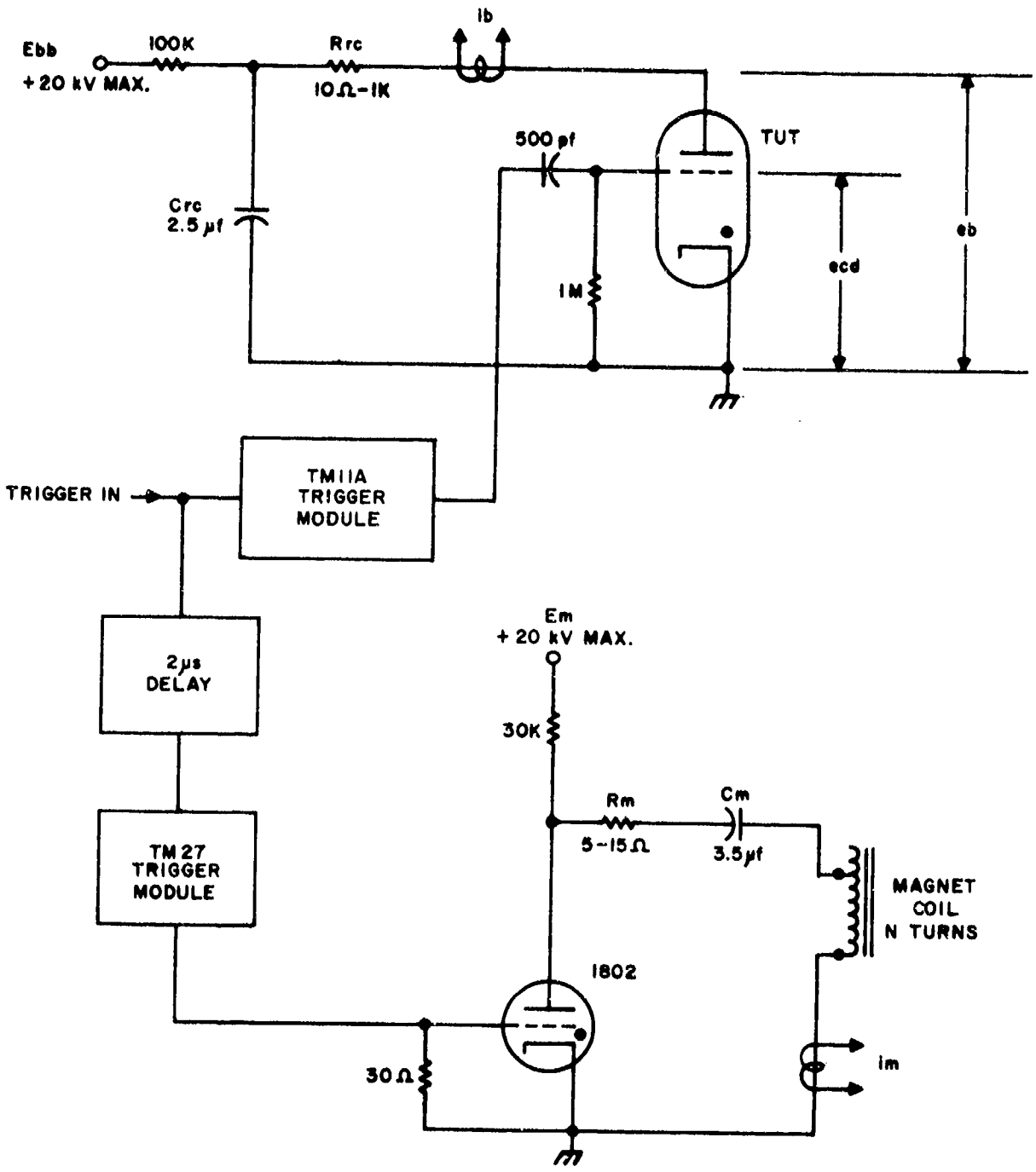

Figure 2. Circuit Used to Determine Magnetic Field Required for Interruption.

The peak current in the TUT, ib, was monitored with a calibrated current measuring transformer placed in the anode lead of the TUT, which transformer thus monitored the sum of the cathode current and any current which flowed through the grid and out of the anode-grid region.

The peak magnet current, im, to which the peak magnetic field is proportional, was monitored with a calibrated current measuring transformer as shown in Figure 2. Independent testing had established that level of im for which the magnet core saturated, and that current level was avoided.

A time delay was introduced as shown such that the magnetic field was not applied to the interaction region until about two microseconds after the initiation of a discharge within the TUT.

The instantaneous anode voltage of the TUT, eb, and the voltage drop of the interaction column, ecd, were monitored with calibrated and frequency-compensated high voltage probes. (The column drop was assumed equal to the grid-cathode drop.)

Observation of eb and ib provided an indication of the effect of the magnetic field on the discharge, and the magnet supply voltage, Em, was adjusted until the magnetic field required for interruption, Bq, was established. Bq was defined as being that field for which the current in the TUT was alternately extinguished or nearly extinguished since it was found that this condition could be achieved with reasonable regularity and independently of other operating conditions.

An arbitrary but representative sample of the data taken with the circuit of Figure 2 is shown in Figure 3, where the upper, center, and lower traces represent eb, im, and ib, respectively. Note that eb is initially equal to epy, drops to etd upon triggering of the RSI, and then returns to high voltage when ib is extinguished by the magnetic field. The voltage eb does not return to epy because ib has removed some of the charge from Crc and the charging resistor (30K) is too large to permit a rapid recharge of Crc. Notice that the trailing edges of both eb and ib have finite slopes; this fact implies that the RSI actually passes through an operating region wherein its incremental impedance assumes discrete values. Thus the RSI is neither a short nor

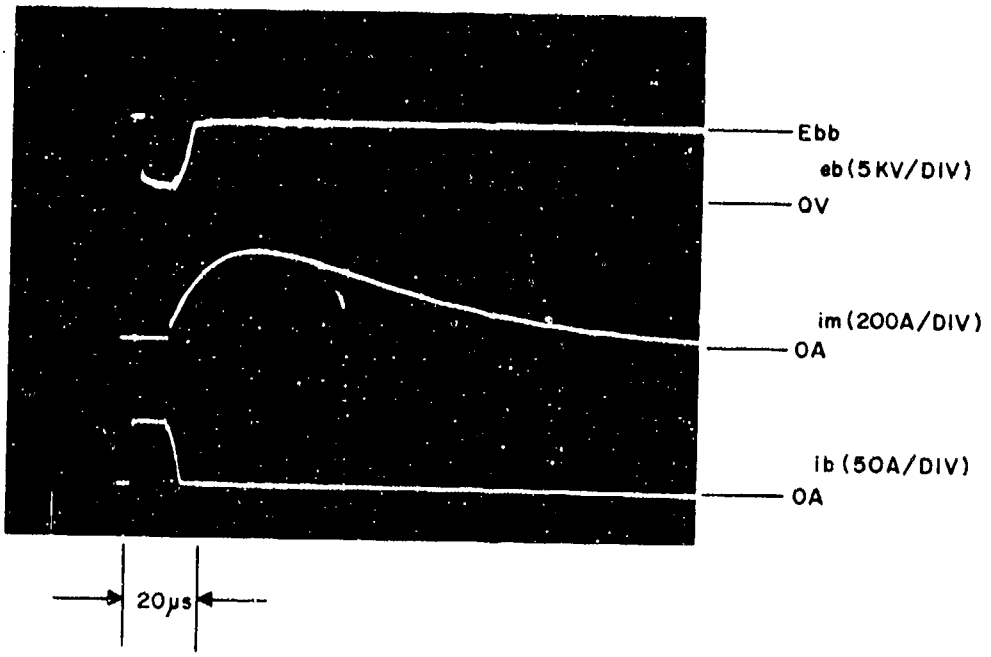

Figure 3. Typical RSI Waveforms in the Absence of Restrike (RSI 10D, Ebb = 5 kV, Rrc = 100Ω , Pulse Rate = 50 pps).

an open circuit during its opening transition. Note also that the RSI appears to have changed its state prior to the peak of the magnetic field. This observation implies that decreasing the rise time of the magnetic field might improve the switching efficiency of the RSI, and subsequent testing verified this supposition, as discussed in subsection 4, part d, of this section.

(2) Determination of Steady-State Tube Drop

Figure 4 shows the circuit used to determine etd, the steady-state tube drop. The anode supply voltage, Ebb, could be continuously varied at will up to 20 kV and two different pulse forming networks were used. One network had an impedance of 42 ohms and a pulse width of 1 μs for investigations of etd at normal thyratron current levels. The other had an impedance of 600 ohms and a pulse width of about 7 μs for investigations of etd at the current levels appropriate for "normal" operation of an RSI. In each case, the load resistor R1 was chosen to provide a slightly negative voltage at the anode of the TUT after the main discharge of the PFN. The peak tube current, ib, was monitored in the same manner as the circuit of Figure 2 and the tube drop measurements were taken at the time corresponding to the midpoint of the current pulse.

The network shown within the dotted lines in Figure 4 was used in conjunction with a calibrated and frequency-compensated probe and an oscilloscope to obtain the actual tube drop data. The measurement of eb, the instantaneous voltage across the TUT, is complicated by the fact that prior to the triggering of the TUT, eb is equal to the peak forward anode voltage, epy. After triggering and commutation, eb is equal to the steady-state tube drop, etd, which is materially less than epy. Thus one is faced with a measurements situation where the dynamic range of the measuring scheme is of great importance. Previous experience with a high voltage probe located directly at the anode of the TUT has shown that such probes may be voltage sensitive, i.e., the attenuation of the probe may be a function of the voltages being measured. Furthermore, the oscilloscope sensitivity which is appropriate for accurate determination of etd results in severe overdriving of the oscilloscope's vertical amplifier in the presence of a signal corresponding to epy.

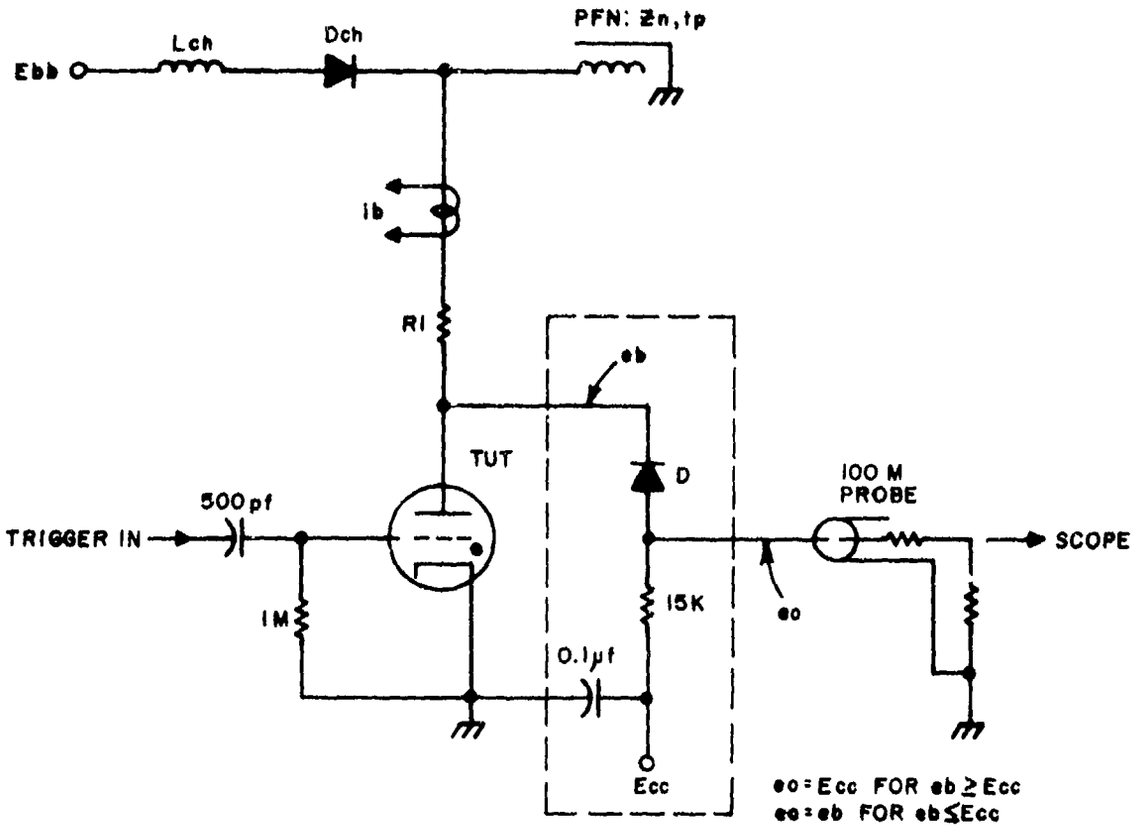

Figure 4. Circuit Used to Determine Steady-State Tube Drop.

To overcome these problems, the diode, D (Figure 4), was used in conjunction with a diode bias supply, Ecc (a positive voltage), and a 15 K diode load resistor as shown. (The 0.1 μF capacitor served only as a filter.) For values of eb greater than Ecc (e.g., eb = epy), the measuring circuit's output voltage, eo, was equal to Ecc because the diode was biased off. For values of eb less than Ecc (e.g., eb = etd), eo was equal to eb because the diode was biased on (the diode drop was neglected). By varying Ecc from zero to large positive values while observing the waveform of eo, one could determine that level of Ecc which was adequately high to reliably measure etd, since higher values of Ecc would result in no change in the portion of the waveform of eo which corresponded to etd.

Representative data obtained in this fashion are shown by the oscillograms of Figure 5. The upper traces show the waveform of eo and the lower traces show the tube current. Note from Figure 5a that the entire waveform of eo (including the negative portion, which is of no particular interest) produces only about 1 cm of oscilloscope deflection. Thus the oscilloscope's sensitivity may be increased by an order of magnitude without overdriving the amplifier during the time of interest. In both Figures 5a and 5b, the bias voltage of 1600 volts and the tube drop of 800 volts can be discerned. Furthermore, the probe never "sees" a voltage greater than 1600 volts during the period of interest, in spite of the fact that epy was 25 kV for the case shown. The technique described here is thus suitable for accurate measurements of etd in the presence of high values of initial anode voltage.

d. Magnetic Fields Required for Interruption

(1) Interrupting Magnetic Fields for Each Tube

Figures 6 through 14 show the results of tests to determine the magnetic fields required to interrupt discharges in each member of the RSI 10 series. In general, data were obtained using the same magnetic field rise time and tube pressure in each case. The load resistance of the fault network, Rrc (Figure 2), was adjusted between 20 ohms and 100 ohms to observe the effects of different values of ib for a given value of Ebb. For tubes having both long and short chutes, data were obtained first with the IXB force directed into one set of chutes, and then with the field reversed. For tubes

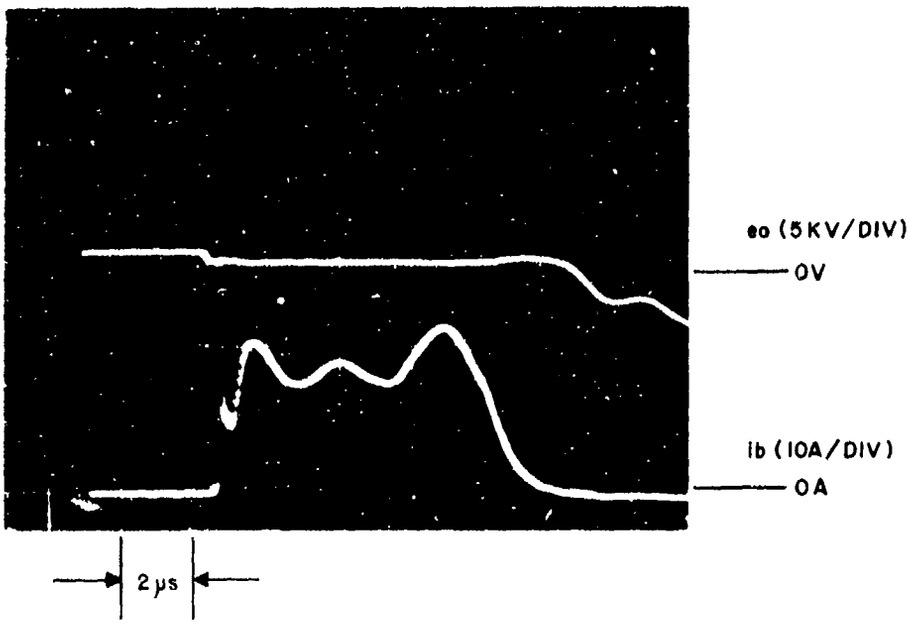

(a)

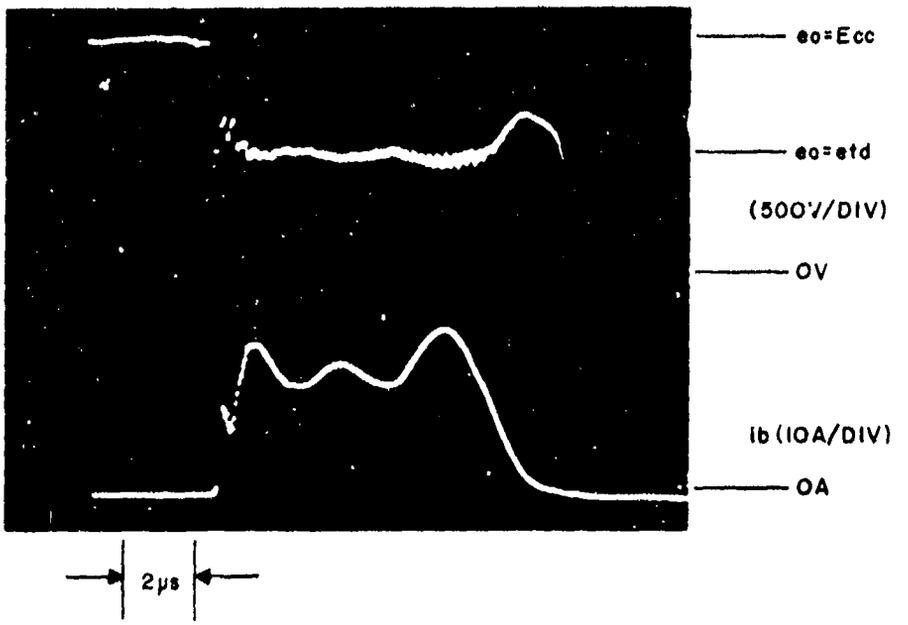

(b)

Figure 5. Typical Tube Drop Waveforms (RSI 10DD, epy = 25 kV, Zn + Rl = 1100 Ω, Pulse Rate = 50 pps).

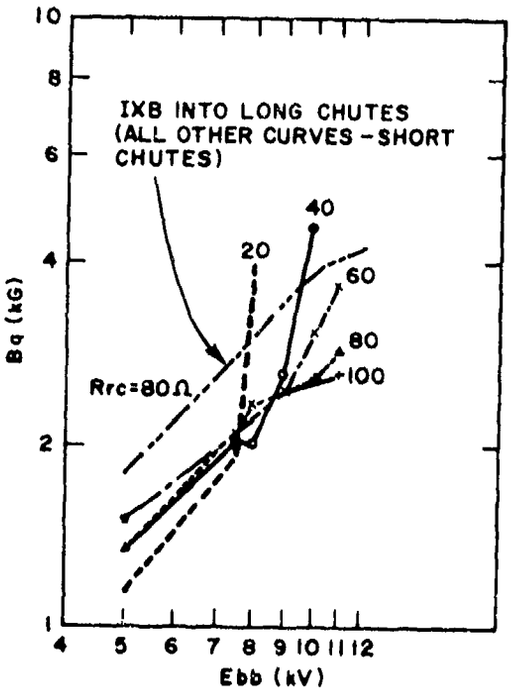

Figure 6. Interruption Characteristics, RSI 10A (p = 0.3 torr; N = 10).

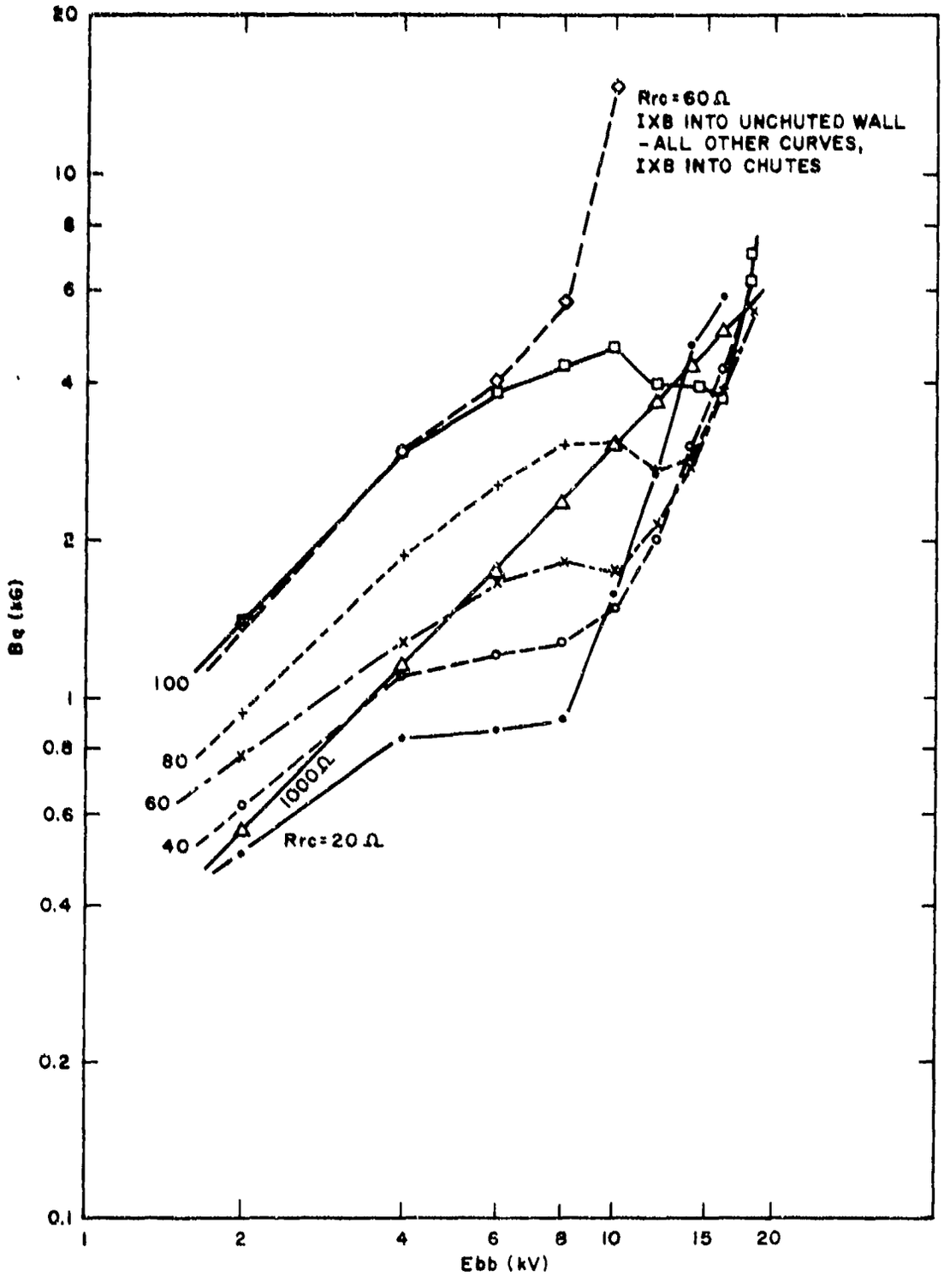

Figure 7. Interruption Characteristics, RSI 10B (p = 0.3 torr; N = 10).

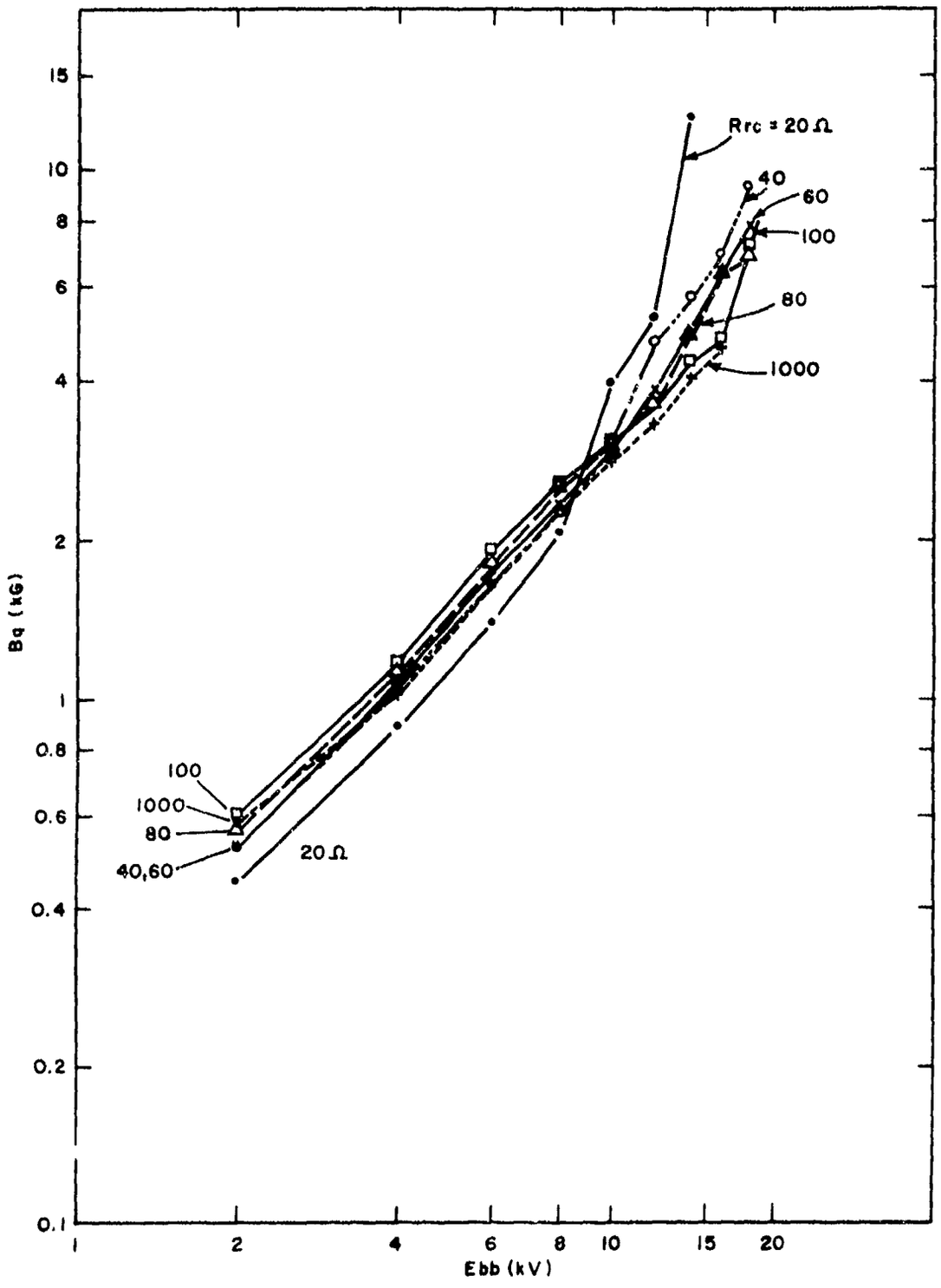

Figure 8. Interruption Characteristics, RSI 10C (p = 0.3 torr; N = 10; IXB into Short Chutes).

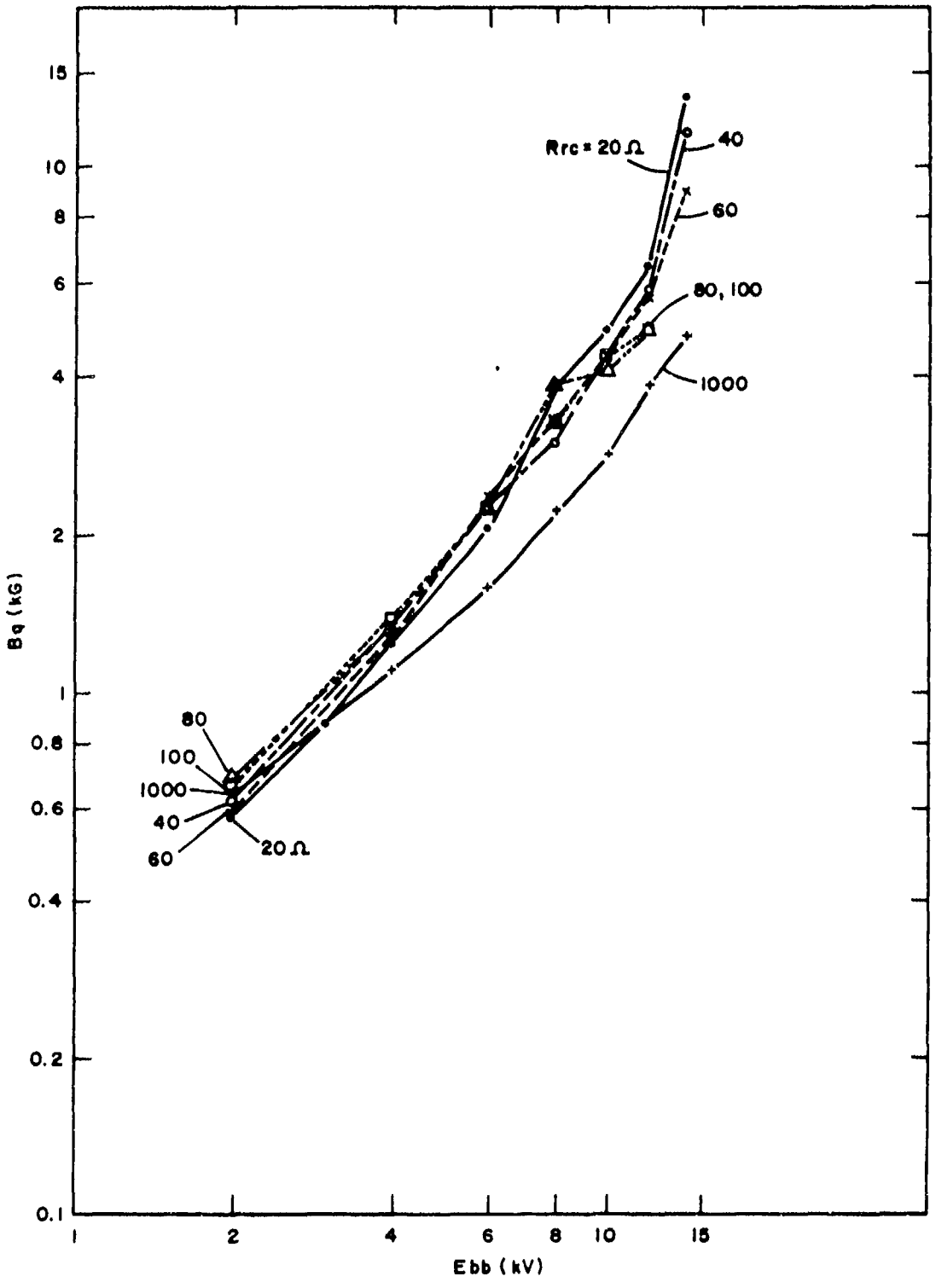

Figure 9. Interruption Characteristics, RSI 10C (p = 0.3 torr; N = 10; IXB into Long Chutes).

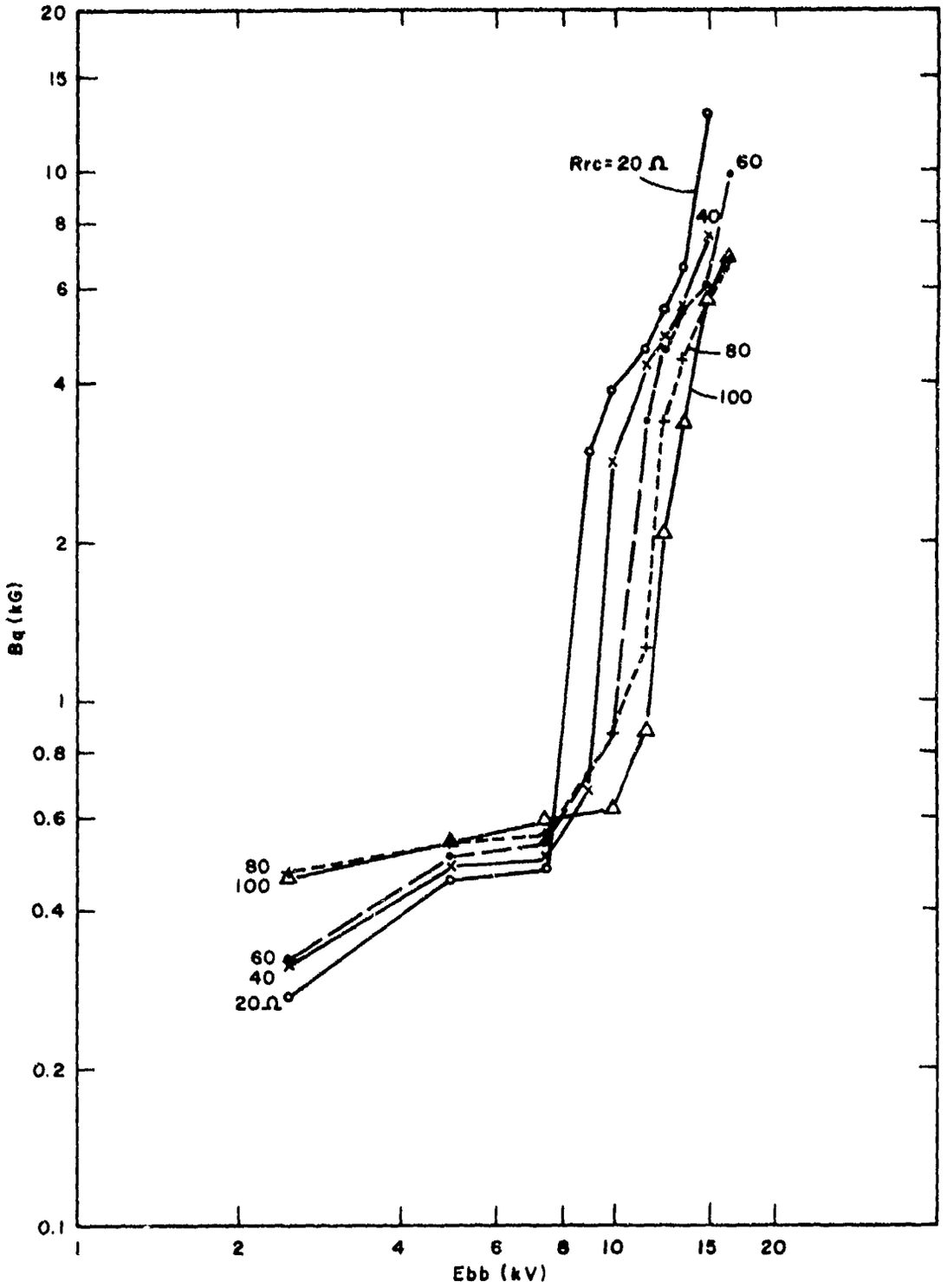

Figure 10. Interruption Characteristics, RSI 10D (p = 0.3 torr; N = 10; IXB into Short Chutes).

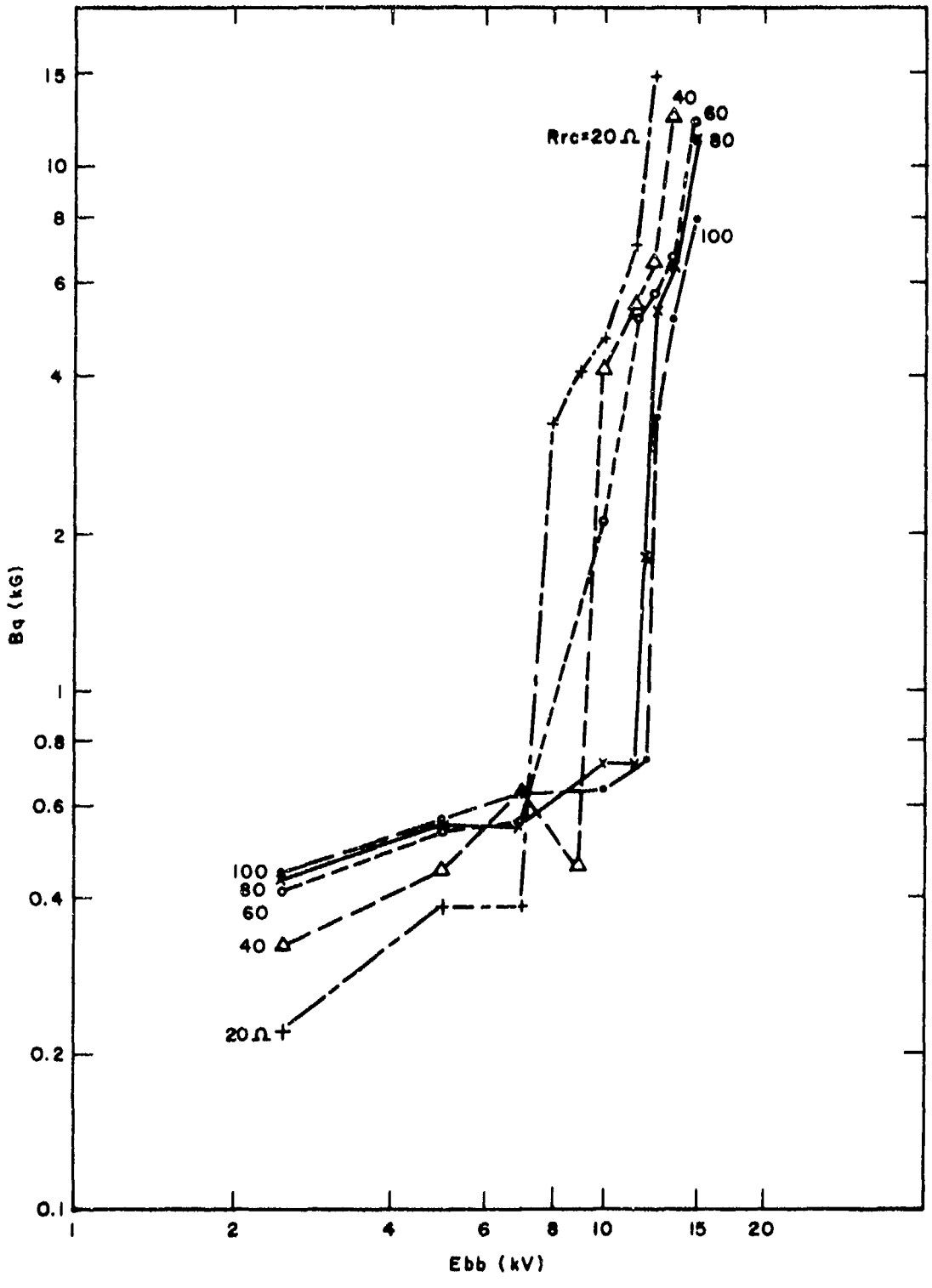

Figure 11. Interruption Characteristics, RSI 10D (p = 0.3 torr; N = 10; IXB into Long Chutes).

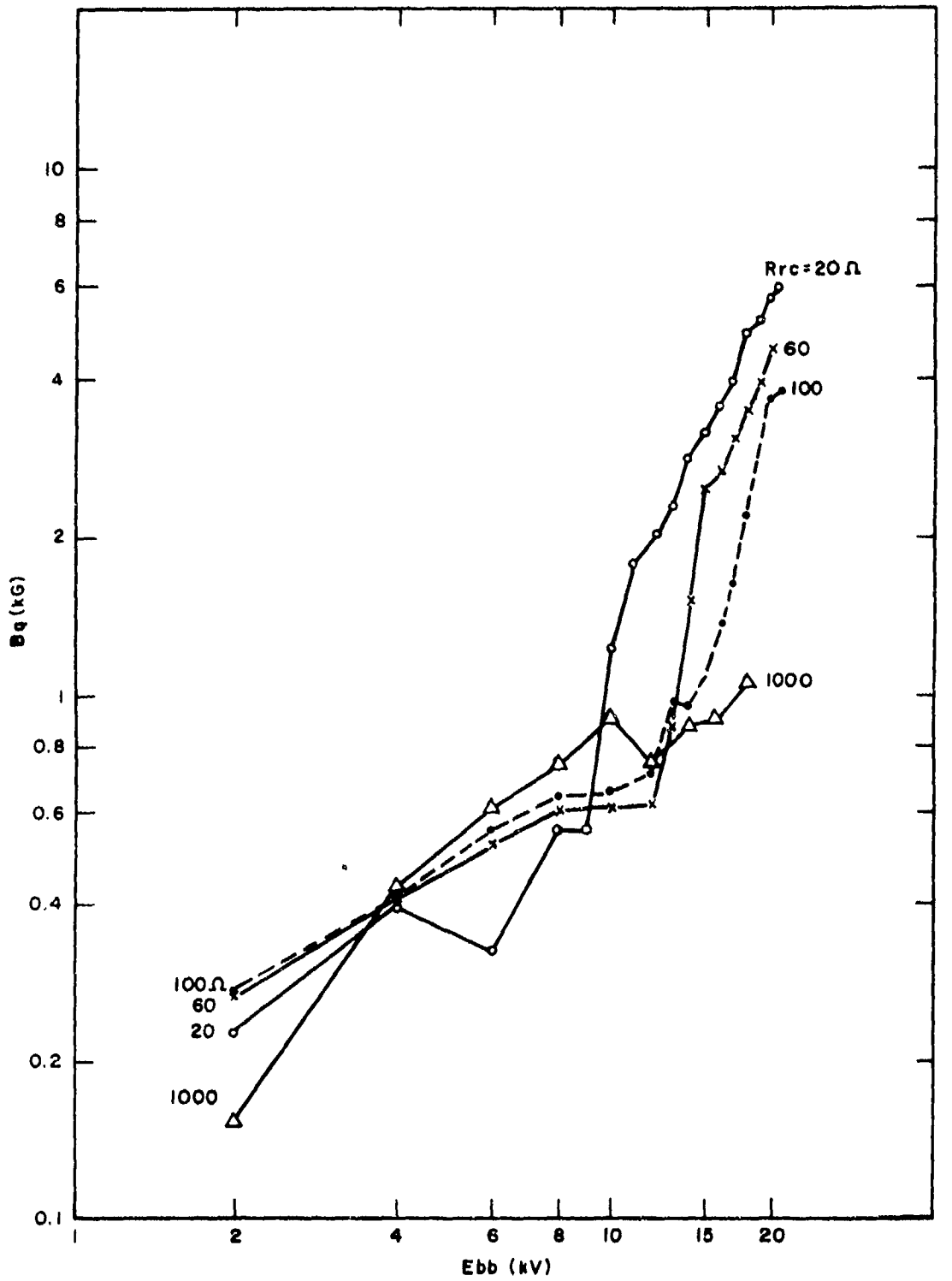

Figure 12. Interruption Characteristics, RSI 10DD (p = 0.3 torr; N = 10; IXB into Short Chutes).

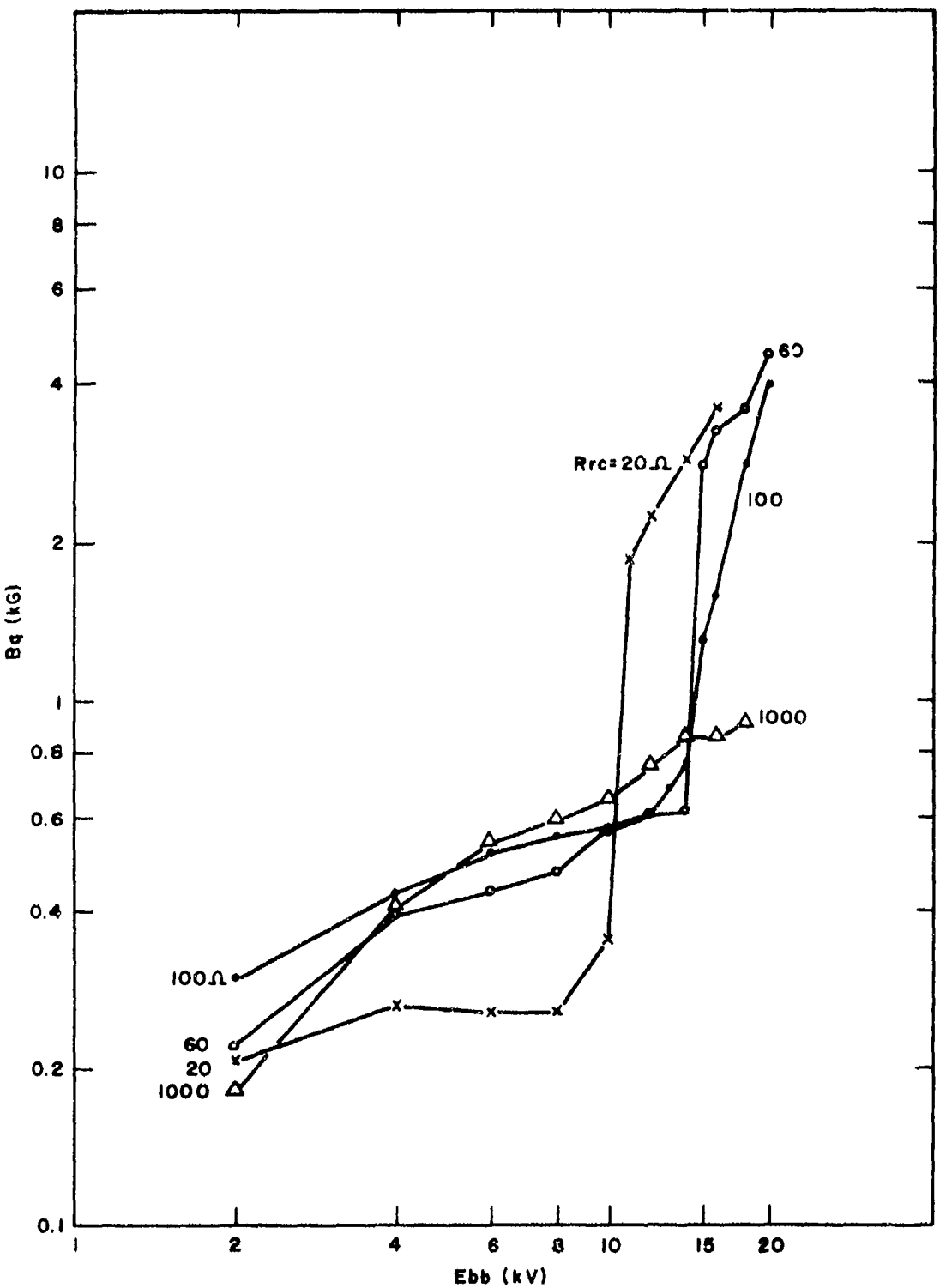

Figure 13. Interruption Characteristics, RSI 10DD (p = 0.3 torr; N = 10; IXB into Long Chutes).

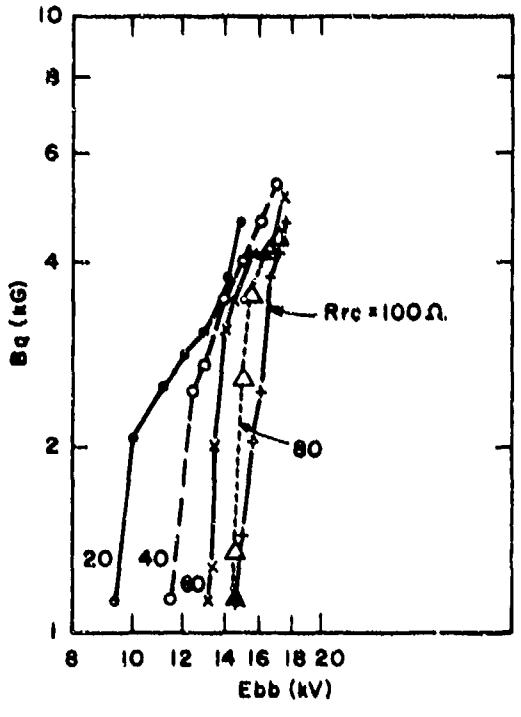

Figure 14. Interruption Characteristics, RSI 10E (p = 0.3 torr; N = 10; IXB into Chutes).

having a smooth wall, data were obtained first with the IXB force directed into the chutes, and then with the field reversed such that the IXB force was directed against the smooth surface. (The RSI 10E showed evidence of arcing in the interaction channel when the IXB force was directed against the smooth surface, and meaningful data for this tube in this mode could not be obtained.) As discussed further in this section, it soon became evident that the tubes performed better with IXB directed into the short chutes (or away from the smooth surface in tubes so equipped), so the data as shown in Figures 6 through 14 are in general more complete for these favored modes of operation.

Many observations and conclusions result from a perusal of the various curves of Figures 6 through 14, so it is well to examine a representative set of curves in detail as is done below.

(2) Modes of Operation

Figure 15 shows again the interruption characteristic for the RSI 10D with the IXB force directed into the short chutes. The curves have been sectioned into regions for purposes of the discussion that follows.

The RSI operated in at least two modes (Regions 1 and 3 of Figure 15), separated by a transition region (Region 2) wherein Bq increased rapidly with increasing Ebb and also became heavily current-dependent. In the lower power region (Region 1), operation at higher currents reduced the field required to interrupt the discharge at a given Ebb, while in the higher power and transition regions (Regions 2 and 3), the reverse was true. In Regions 1 and 3, the curves exhibit a definable slope and stable operation (repeatable Bq) was readily achievable, but in Region 4, stable operation was difficult to achieve and the tube showed some evidence of arcing in the interaction channel. The various trends exhibited by the RSI 10D and shown in Figure 15 were repeatable for this tube and were also in evidence to varying degrees for each member of the RSI 10 family, as examination of Figures 6 through 14 shows.

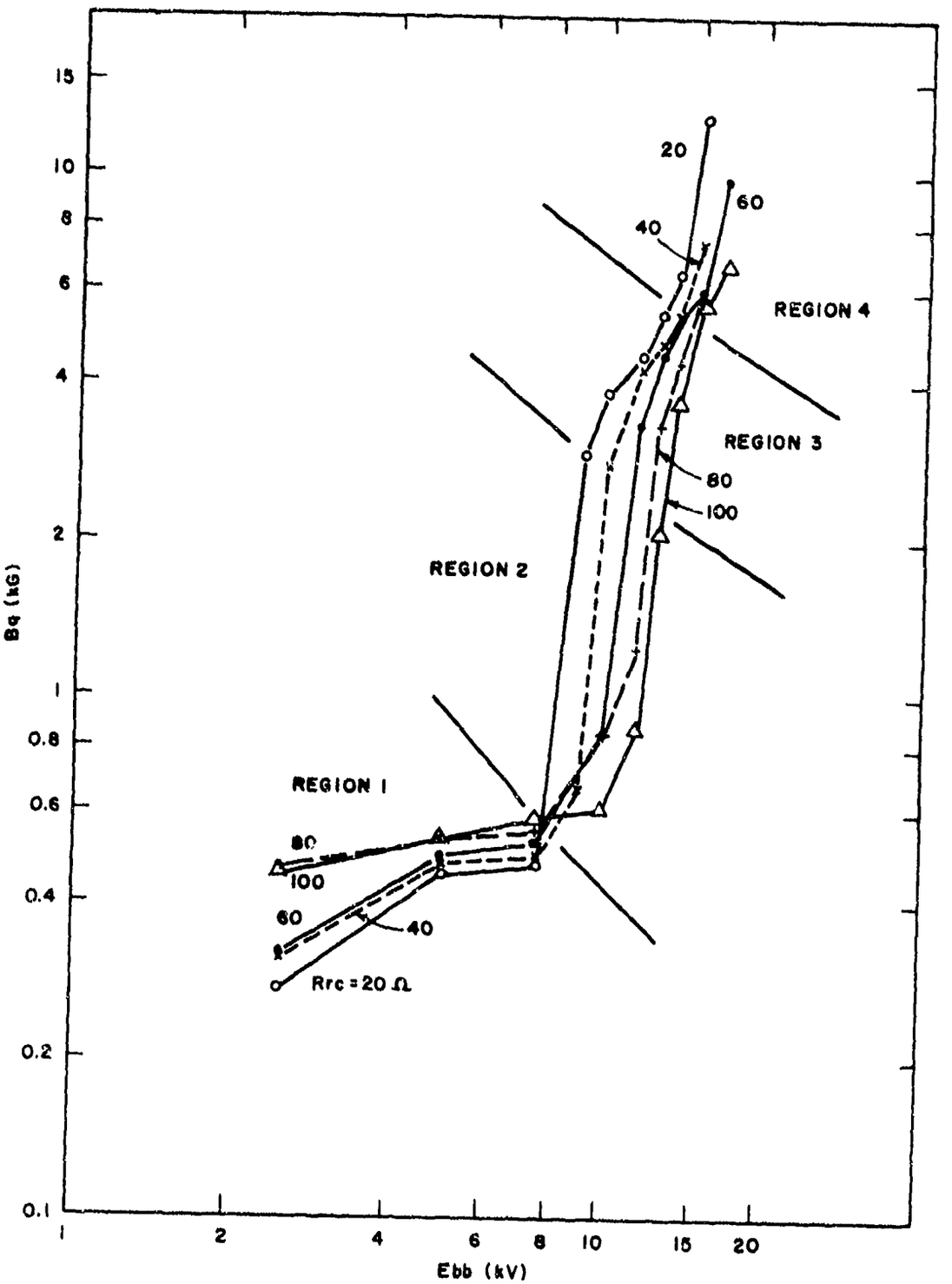

Figure 15. Interruption Characteristics, RSI 10D (p = 0.3 torr; N = 10; IXB into Short Chutes).

It would clearly be desirable to move the breakpoint between Regions 1 and 2 toward higher Ebb, since in Region 1 the magnetic fields required for interruption are nearly an order of magnitude below those of Region 3, and the slopes of Region 1 imply that reliable interruption could be readily achievable over a wide range of power levels with a relatively low magnetic field. Toward this end, the breakpoint between Regions 1 and 2 in Figure 15 was carefully examined by taking many data points in the 8 to 14 kV range of Ebb. In addition, Bq was investigated for values of Rrc equal to 10 ohms and 1000 ohms, and the number of turns of the magnet coil was reduced from ten to four to observe the effects of magnetic field rise time on the field required to achieve interruption. (The effects of tr on Bq are discussed elsewhere in this section and will not be pursued here.) As shown in Figure 16, the data for low (10 ohms) and high (1000 ohms) Rrc follow the trends set by the various other impedance levels.

The response of the RSI 10D was also investigated at various tube pressures and representative data appear in Figure 17. It is seen from Figure 17 that tube pressure has a material effect on Bq only at low Ebb, although some improvement is in evidence for low pressure operation at moderate Ebb, which observation is consistent with the results of previous work.

The overall conclusion from the data shown in Figures 15 through 17 is that the mechanisms for interruption differ significantly depending upon the mode of operation that corresponds to given operating conditions of Ebb and ib, and that the specific nature of these mechanisms is not readily apparent without extensive additional investigation. Reference to the interruption curves for the various tubes (Figures 6 through 14) shows that the geometry of the interaction channel profoundly affects the overall interruption performance on a tube-to-tube basis, and this observation is discussed at length in this section.

(3) Effects of Various Chuting Arrangements on Bq

Figure 18 shows a comparison of the performance of several 10 series RSI's when the IXB force is directed in one case into the long chutes, and in another case into the short chutes. A comparison is also made for the RSI 10B, which had both chuted and unchuted (smooth) surfaces. For all tubes

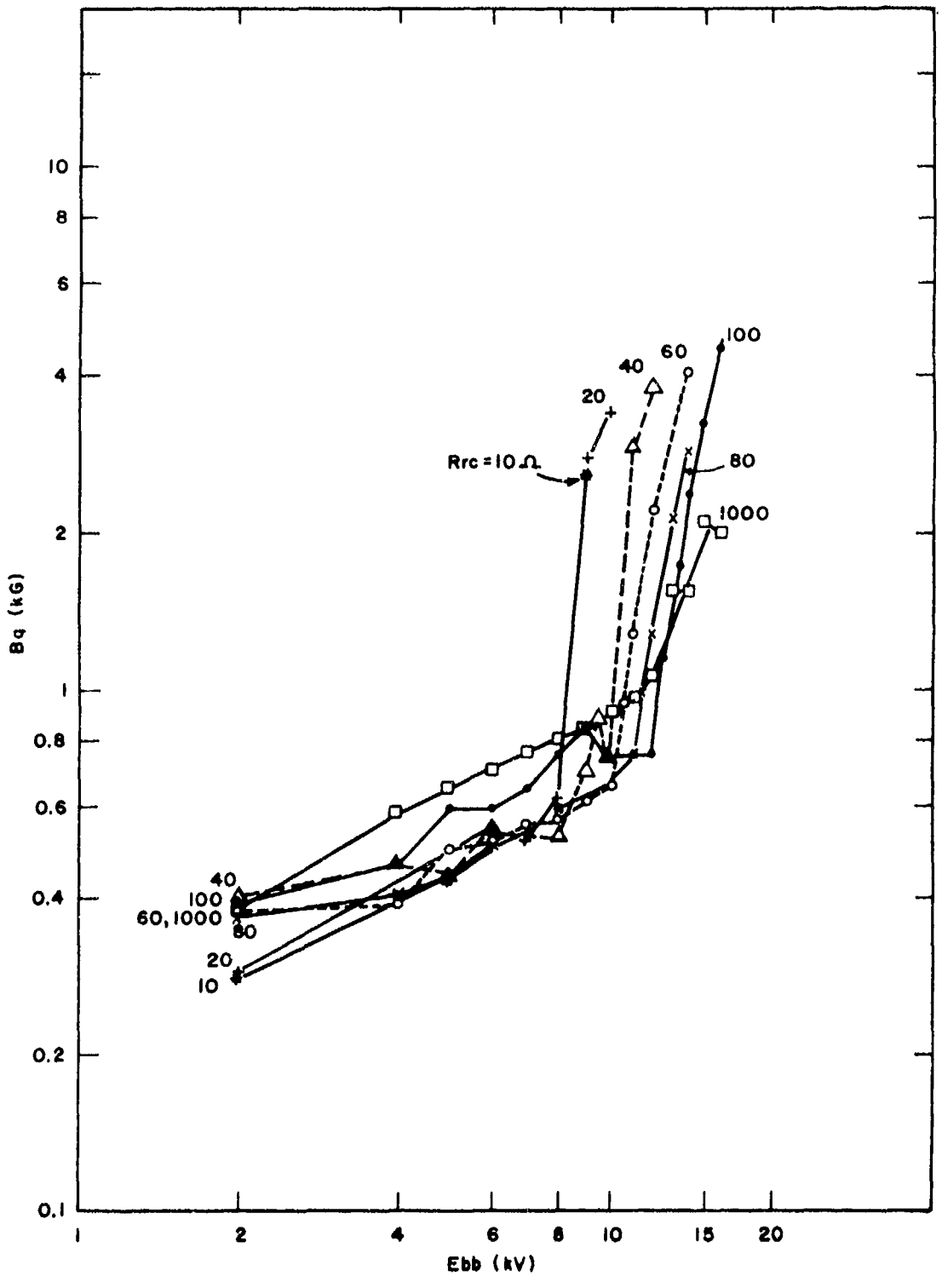

Figure 16. Interruption Characteristics, RSI 10D (p = 0.3 torr; N = 4; IXB into Short Chutes).

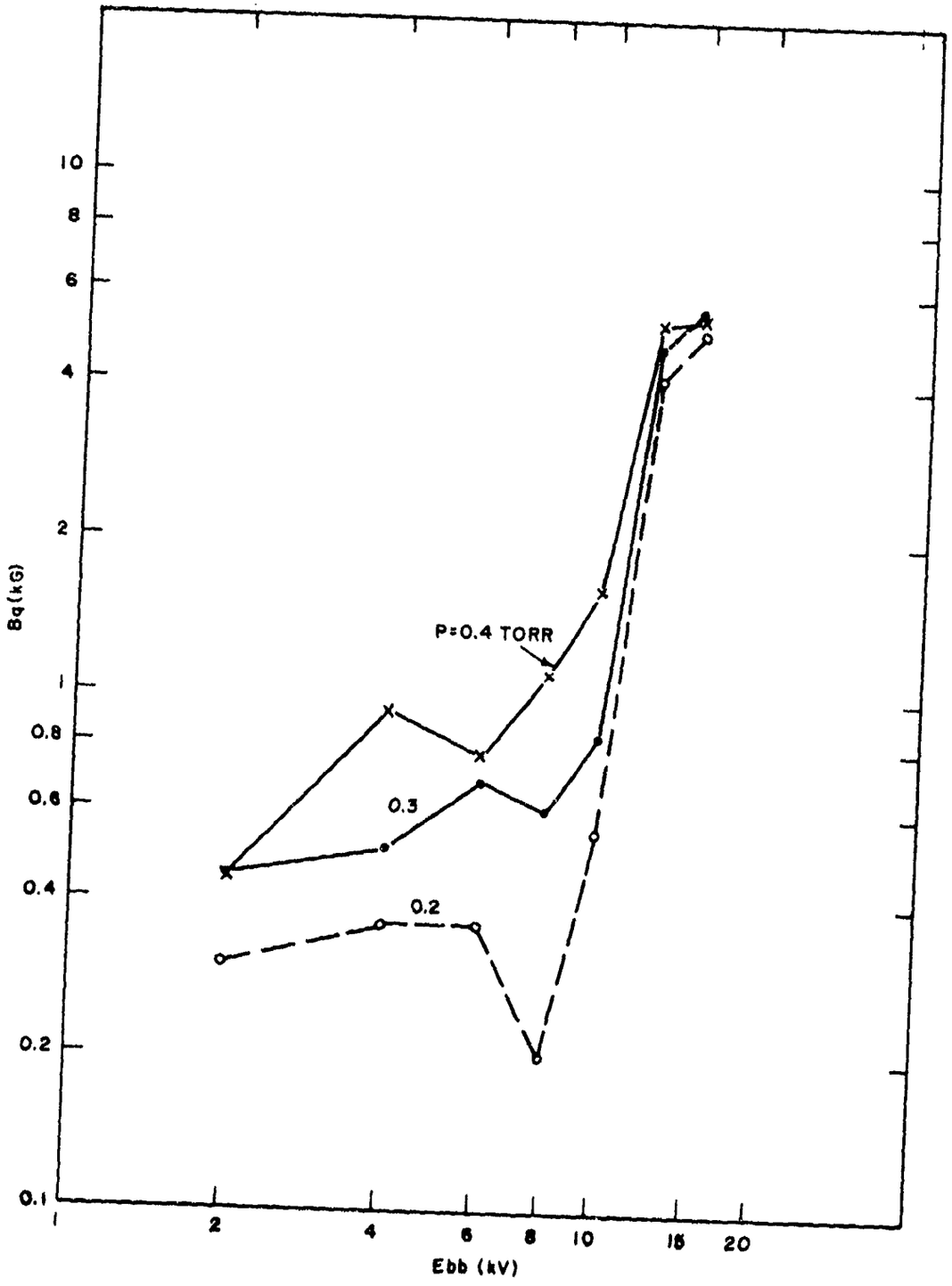

Figure 17. Interruption Characteristics RSI 10D (Rrc = 60 Ω ; N = 10; IXB into Short Chutes).

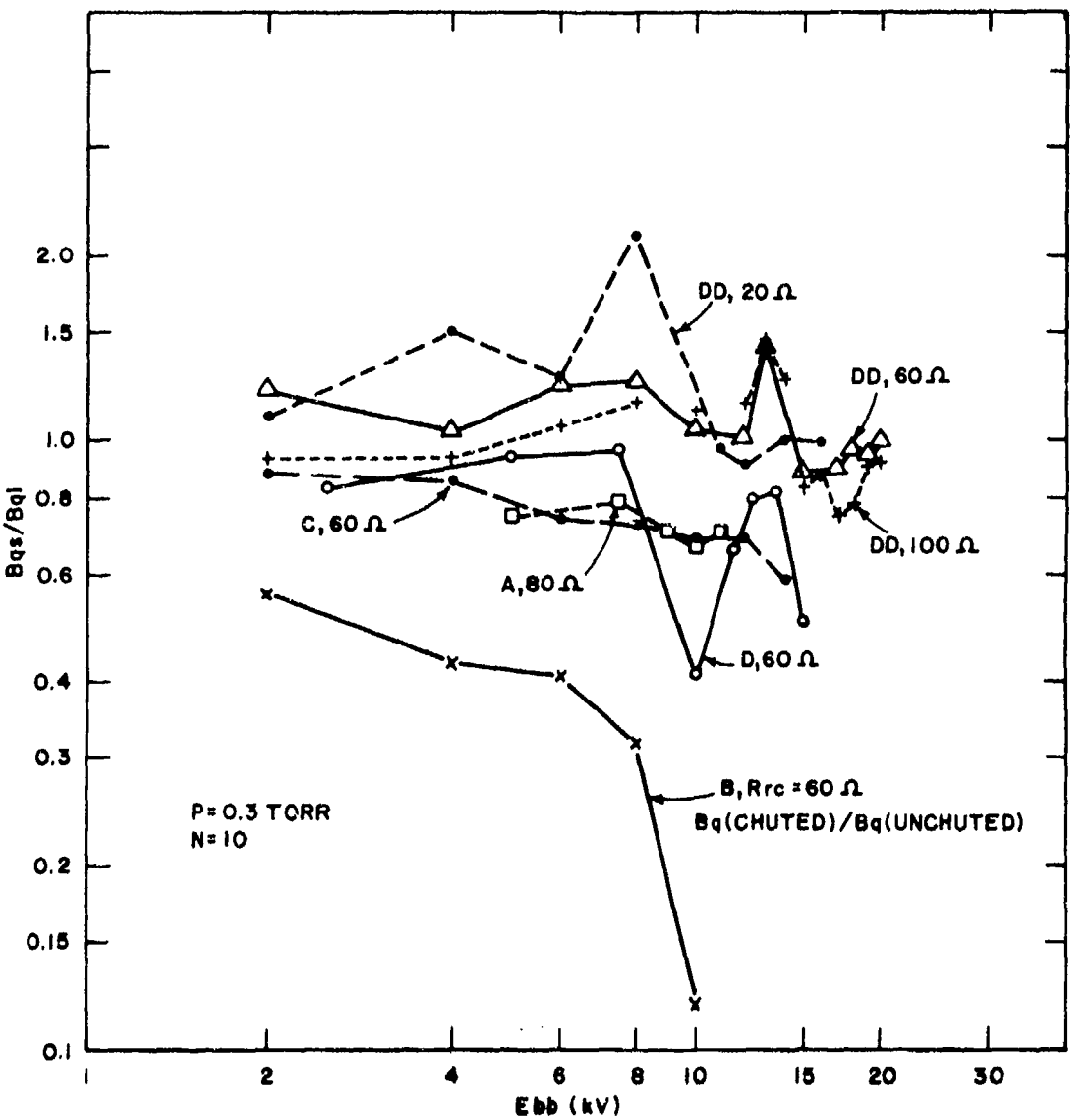

Figure 18. Ratio of Bq for IXB into Short Chutes (Bqs) to Bq for IXB into Long Chutes (Bql), RSI's 10A, B, C, D, DD.

except RSI 10DD, the ratio of Bqs to Bql (as defined in Figure 18) is less than unity, implying that short chutes "work better" than long chutes. In the case of the RSI 10B, chutes work better than no chutes. Even for the DD, the ratio Bqs/Bql is less than unity over the region of interest (Ebb > 15 kV) for the several values of Rrc shown. Two explanations for this phenomenon come to mind: first, that the "wall" at the end of a short chute is helpful in promoting a quench of the discharge; second, that the discharge does not penetrate deeply into the long chutes, and that plasma trapped therein hinders the interruption. In the case of Tube B, the effect is most pronounced. This might at first be construed as being merely representative of the fact that chuted tubes are more efficient interrupters than are unchuted tubes as stated above, but when all tubes are compared (refer to Figure 20), it is seen that Tube B is in fact one of the better overall performers, as is Tube E, another tube having a smooth surface. The conclusion is that potential gas reservoirs are best avoided and this point is discussed further in this section.

(4) Effects of Magnetic Field Rise Time

As discussed in subsection 1, part c, of this section, it has been observed that RSI's interrupt at a point in time prior to the peak of the magnetic field, which observation leads to the theory that decreasing tr should reduce Bq. Representative data which show this to be the case for the region of interest (high Ebb) appear in Figure 19, where both the absolute values of Bq and the ratio of the appropriate Bq's is shown for two different tubes, each of which was operated at two different rise times. The conclusion is that efforts to improve the performance of the magnet circuit are worthwhile in terms of overall RSI system performance.

(5) Comparison of the 10 Series RSI's

Figure 20 shows the interruption characteristics for each member of the RSI 10 family of tubes. Data is shown only for the IXB force directed into the short chutes (or into the chutes in the case of tubes having unchuted surfaces), since in general this was the preferred mode of operation. The curves of Figure 20 apply for Rrc = 20 ohms, which value was chosen first because it corresponds to the fault currents which are consistent with the

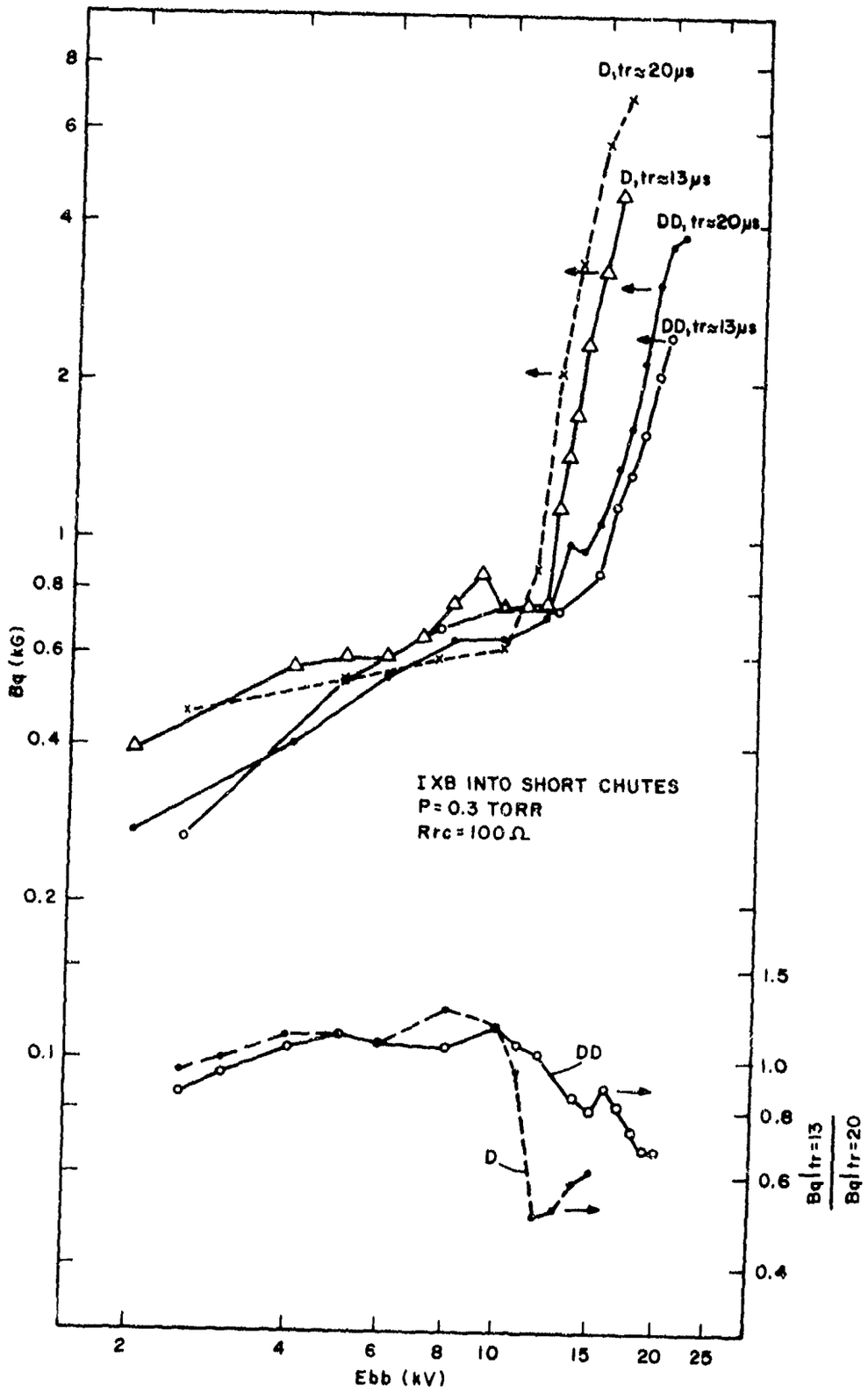

Figure 19. Effect of Magnetic Field Rise Time (tr) on Bq, RSI 10D and RSI 10DD.

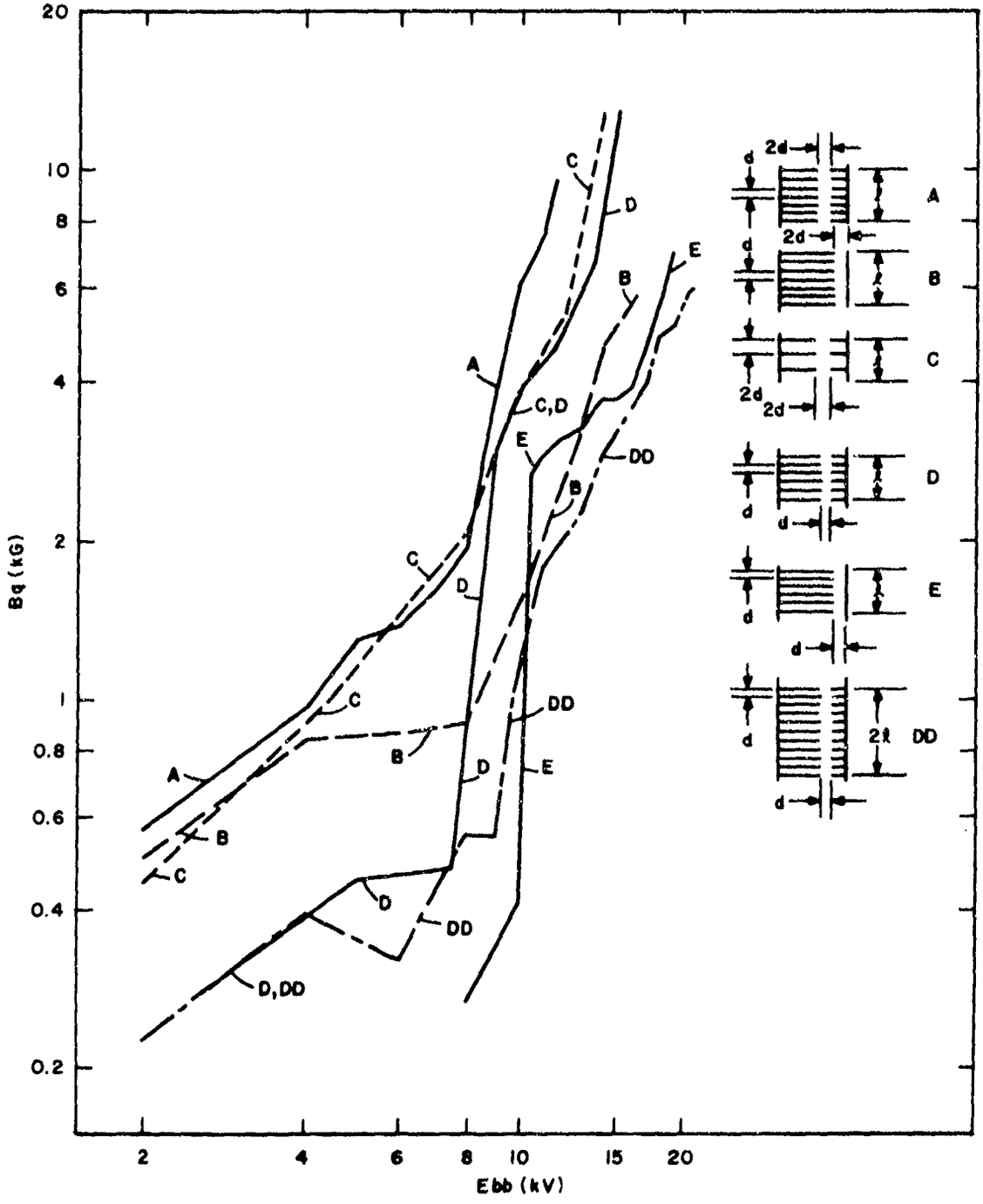

Figure 20. Interruption Characteristics, RSI 10 Series. p = 0.3 torr, N = 10 (tr = 13 μs), Rrc = 20 Ω (IXB into Short Chutes for Chuted Tubes; IXB into Chutes for Tubes with a Smooth Wall).

goals of the Program, and second, as an examination of Figures 6 through 14 shows, because the true behavior of any given tube is best revealed by the tube's performance at higher currents. Nevertheless, when considering Figure 20, reference should also be made to the detailed curves for the tubes in question, since marked differences do exist as a function of fault current for any given tube.

From Figure 20, the RSI 10DD clearly emerges as the most successful of the 10 series tubes. Furthermore, and as discussed further in this section, the specially designed holdoff section used with this tube provided a low holdoff section voltage drop and yet operated reliably at epy = 30 kV. At 25 kV, 18.5 A, the DD operated with a total tube drop of only 830 volts, or 3.3% of epy.

From Figure 20 and a comparison of the pertinent detailed curves, one would choose the E over the B and the D over the A. The conclusion is that channels of narrow I.D. are in general to be preferred, an observation which is consistent with previous data. Again from Figure 20, one would choose the E over the D and the B over the A. It appears that the presence in the interaction channel of an unchuted surface, along which the uninterrupted discharge most likely flows, enhances the interruption process by precluding the existence of a reservoir which can supply plasma to the discharge. Finally, from Figures 8 and 20, the C, with its relatively open internal structure, behaves as though it were an unchuted tube. At low Ebb (and correspondingly low ib), the C behaves like the two other wide-bore tubes (the A and the B). At high Ebb and ib, it behaves like the D. This is reasonable since both the bore and the inter-chute spacing of the C are double those of the D, i.e., the scaling of the two tubes is the same.

Based on the above observations and other miscellaneous data, and without speculation as to the physical causes for all of the observed phenomena, one would conclude that the optimum tube would:

1. be of narrow bore;
2. contain both an unchuted and a chuted surface against which latter surface the discharge is driven;

3. contain a large number of relatively short and closely spaced chutes;
4. consist of multiple, folded interaction sections;
5. contain a holdoff section specifically designed to minimize the total tube drop;
6. operate at relatively low pressure;
7. contain a gradient grid for operation at epy up to 50 kV.

The above conclusions have been considered in the design of the RSI 12 series (the five exploratory development tubes), as discussed in Section 4.0.

e. Steady-State Tube Drop

(1) Standard Thyratron - EG&G Type HY-6

It has been shown that appending a standard thyratron holdoff section to an interaction column does not materially alter the voltage drop of the section. All of the 10 series RSI's except Type DD were equipped with a holdoff section identical to that of a standard production thyratron, EG&G Type HY-6. The total tube drop of an HY-6 was measured using the technique described in subsection 2, part c, of this section, and the results of this investigation are shown in Table 2.

From Table 2, it is seen that, at all tube pressures, etd increases only moderately with increasing epy (due probably to the corresponding increase in ib), and that an optimum pressure for minimum tube drop also exists. In all cases, the deviation of etd from its average value is relatively small, and thus unlikely to dominate the performance of an RSI. The conclusion to be drawn from the data shown in Table 2 is that RSI's may be designed with other considerations (e.g., the optimum pressure for minimum Bq) taking precedence over the drop of the holdoff section.

Table 2. Total Tube Drop of HY-6 Thyratron at Various Tube Pressures and Power Levels (Zn + Rl = 1100Ω).

epy (kV)	etd (V) at P = 0.12 torr	etd (V) at P = 0.29 torr	etd (V) at P = 0.60 torr
5	120	110	120
10	122	115	125
15	125	120	130
20	128	122	140
25	132	130	140
30	140	140	140
35	140	140	140

Tube Drops Averaged Over Pressure

epy (kV)	etd (V)
5	117
10	121
15	125
20	130
25	134
30	140
35	140

Tube Drops Averaged Over Voltage

P (torr)	etd (V)
0.12	130
0.29	125
0.60	134

Average of all tube drops: 130 volts.

(2) Modified Holdoff Structures - RSI 11 Series

In spite of the discussion above, it is of course advantageous to establish the voltage drop of the holdoff section at the minimum level that is consistent with a reliable holdoff capability. In general this is accomplished by "opening up" the structure, i.e., by increasing the anode-grid gap, grid aperture area, and the grid-grid baffle spacing. This procedure tends to reduce the holdoff capability of the structure, so low etd and high epy are in general inconsistent requirements.

Modifications were made to two standard HY-6 holdoff structures as shown in Figure 21, and the two tubes thus created were designated RSI 11A and RSI 11B. These tubes were not in fact RSI's but rather thyratrons modified as Figure 21 shows.

Tube drop data for both the 11A and 11B are shown in Tables 3 and 4, respectively. The drops of both tubes were somewhat less than those of the HY-6 structure, as a comparison of Tables 2, 3, and 4 shows. However, holdoff capability was lost for the RSI 11A in that the tube operated satisfactorily only at low pressures. The RSI 11B was a success in that its drop was the lowest of the three structures in the pressure region which corresponds to a good compromise between low Bq and reasonable triggering characteristics (0.22 torr - Table 4), and yet the tube reliably held off 30 kV over all reasonable values of gas pressure. The 11B type of structure was used on the RSI 10DD, which, owing to its double-length interaction column, exhibited the highest column drop of the 10 series RSI's. As discussed below, the 11B type of holdoff section functioned well and thus contributed to the overall good performance of the RSI 10DD.

(3) RSI 10 Column Drops

Typical values for ecd, the steady-state drop across the interaction column, were found to average about 300 volts for Types A, B, C, and E. A typical value for Type D was 425 volts, while that for Type DD (twice the column length of the D but otherwise identical) was about 850 volts when measured under the same conditions. Subsequent (and more accurate) measurements of ecd for the DD tube showed an average column drop of 800 volts. For

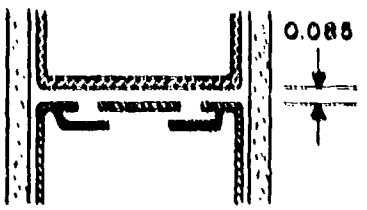

STANDARD HY-6
ANODE-GRID GEOMETRY
(USED IN ALL 10 SERIES
TUBES EXCEPT TYPE 00)

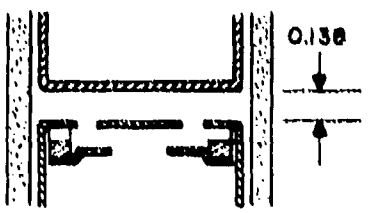

RSI 11B
AND
RSI 100D

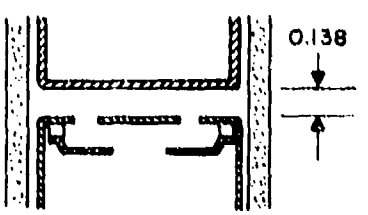

RSI 11A

	Anode-Grid Gap	Grid Aperture Width	Grid-Grid Baffle Spacing	Grid Baffle Aperture	Fill Pressure (microns)
HY-6	0.085	0.092	0.070	0.328	425
RSI 11A	0.138	0.120	0.150	0.328	300
RSI 11B	0.138	0.120	0.106	0.328	300
RSI 100D	0.138	0.120	0.106	0.328	400

Figure 21. RSI Holdoff Sections.

Table 3. Total Tube Drop of RSI 11A at Various Tube Pressures and Power Levels ($Z_n + R_1 = 1100\Omega$).

epy (kV)	etd (V) at P = 0.095 torr	etd (V) at P = 0.14 torr	etd (V) at P = 0.22 torr
5	120	105	115
10	130	110	117
15	130	115	120
20	135	120	122
25	140	125	*
30	140	130	*

Tube Drops Averaged Over Pressure

epy (kV)	etd (V)
5	113
10	119
15	122
20	126
25	133
30	135

Tube Drops Averaged Over Voltage

P (torr)	etd (V)
0.095	132
0.14	117
0.22	118

Average of all tube drops: 122 volts.

*No holdoff capability under these conditions.

Table 4. Total Tube Drop of RSI 11B at Various Tube Pressures and Power Levels ($Z_n + R_l = 1100\Omega$).

epy (kV)	etd (V) at P = 0.09 torr	etd (V) at P = 0.22 torr	etd (V) at P = 0.55 torr
5	110	100	125
10	115	105	130
15	122	115	130
20	125	120	130
25	130	122	130
30	135	125	130

Tube Drops Averaged Over Pressure

epy (kV)	etd (V)
5	112
10	117
15	122
20	125
25	127
30	130

Tube Drops Averaged Over Voltage

P (torr)	etd (V)
0.09	122
0.22	114
0.55	129

Average of all tube drops: 122 volts.

most tubes, ecd decreases with decreasing pressure over the pressure range of interest, but the change in ecd with pressure is not a dominant effect for the tubes under discussion. Present data thus indicate that column drops of the order of 400 volts per section will be typical of an efficient RSI.

(4) RSI 10DD Tube Drop

As the most efficient (and highest voltage) interrupter among the 10 series tubes, the RSI 10DD was the logical choice for use as a vehicle to study etd, the steady-state tube drop.

Figure 22 shows etd as a function of tube pressure for various values of epy and ib where a relatively low impedance line has been used to permit values of ib more in keeping with usual thyratron operating conditions. Table 5 shows the same type of data for the high impedance line which provides the relatively low values of ib specific to the RSI application. Both Figure 22 and Table 5 show a small decrease in etd with decreasing pressure, but the absolute values of etd are higher in the high current case. These characteristics are emphasized in Figure 23, which shows etd as a function of tube pressure for both the high and low impedance cases. To generate Figure 23, etd was averaged over voltage at each value of P shown, a valid procedure since the currents corresponding to each impedance level differ significantly. Also in Figure 23, the curve for the low impedance case is shown only for the lower pressure region (the region of interest) owing to the relative paucity of data at high P and low Zn as shown in Figure 22. (At high pressure and low Zn, the tube would go into continuous conduction at high epy. To include only the low epy data in Figure 23 would unduly weight the average of etd toward low voltage operation.)

Two conclusions can be reached from Figure 23. First, over the current and pressure ranges under consideration (3-18 A for high Zn; 70-300 A for low Zn), etd increases measurably but not significantly with increasing current; second, as the table of Figure 23 emphasizes, etd also increases with increasing pressure to a measurable but not significant extent.

Table 5. Tube Drops for 600-Ohm Line with R1 = 500 Ohms, RSI 10DD.

Tube Pressure (microns)	epy (kV)	etd (volts)	ib (amps)	Tube Pressure (microns)	epy (kV)	etd (volts)	ib (amps)
115	5.0	950	3.4	380	5.0	950	3.3
	7.5	900	5.6		7.5	920	5.6
	10.0	825	7.5		10.0	920	7.4
	12.5	810	9.6		12.5	920	9.6
	15.0	800	11.5		15.0	920	11.5
	17.5	800	13.5		17.5	920	13.0
	20.0	800	15.5		20.0	920	15.0
	22.5	750	16.5		22.5	900	16.5
	25.0	800	18.5		25.0	900	18.5
160	5.0	920	3.4	480	5.0	1000	3.4
	7.5	900	5.6		7.5	1000	5.4
	10.0	880	7.4		10.0	970	7.2
	12.5	840	9.6		12.5	960	9.6
	15.0	810	11.4		15.0	960	11.5
	17.5	800	13.0		17.5	950	13.0
	20.0	790	15.5		20.0	950	15.0
	22.5	810	16.5		22.5	940	16.5
	25.0	810	18.5		25.0	930	18.5
222	5.0	900	3.4	600	5.0	1050	3.3
	7.5	880	5.6		7.5	1000	5.4
	10.0	920	7.4		10.0	1000	7.2
	12.5	900	9.4		12.5	1000	9.4
	15.0	860	11.2		15.0	1000	11.5
	17.5	850	13.0		17.5	1000	13.0
	20.0	810	15.0		20.0	1000	15.0
	22.5	810	17.0		22.5	970	16.5
	25.0	810	18.0		25.0	—	—
290	5.0	920	3.4				
	7.5	900	5.4				
	10.0	920	7.2				
	12.5	920	9.4				
	15.0	890	11.1				
	17.5	900	13.5				
	20.0	850	15.0				
	22.5	870	16.5				
	25.0	900	18.5				

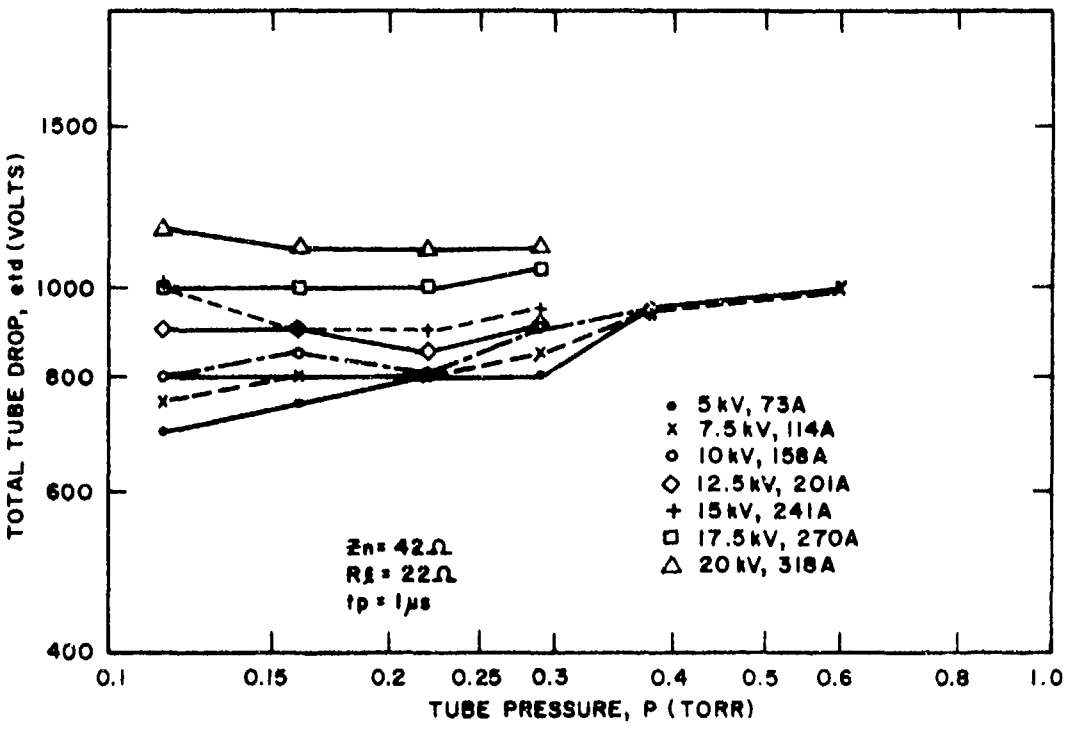

Figure 22. Total Tube Drop as a Function of Tube Pressure, RSI 10DD.

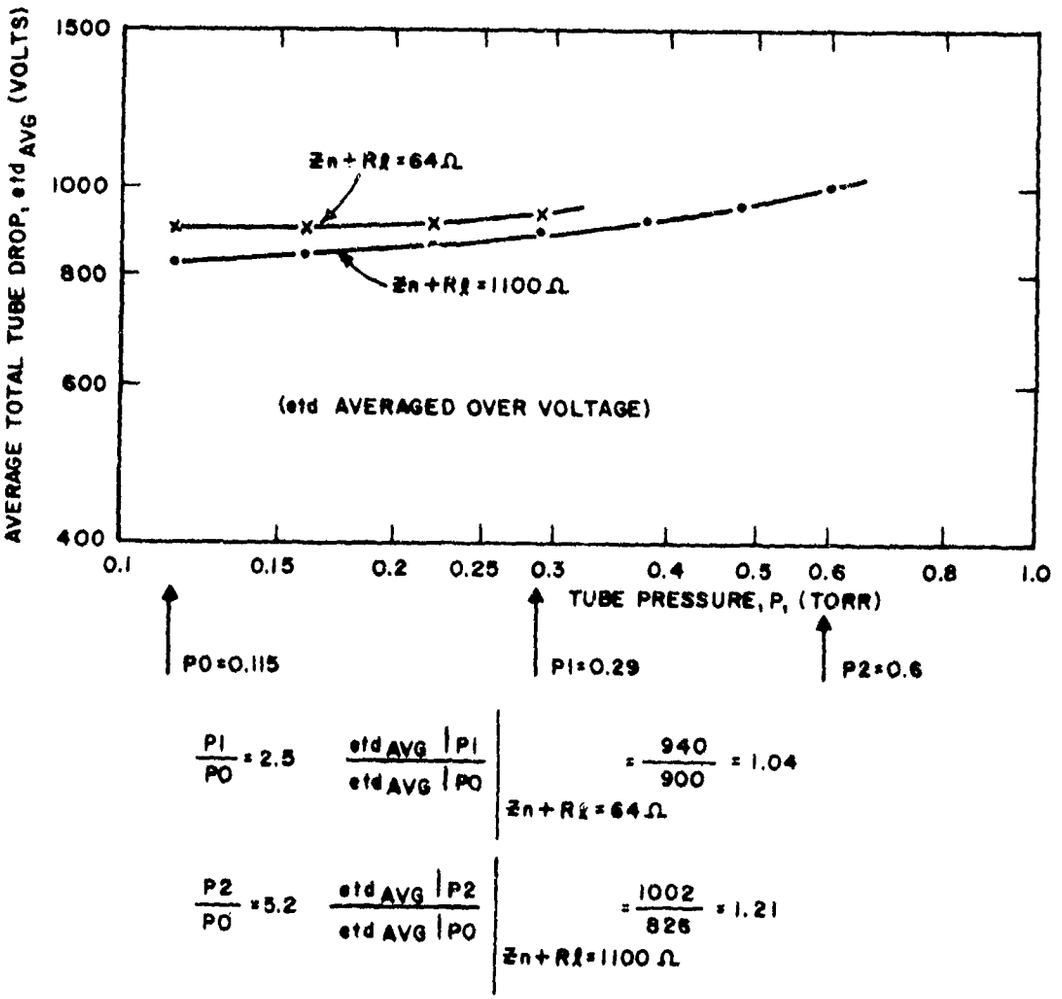

Figure 23. Average Total Tube Drop (etd_{avg}) as a Function of Tube Pressure at High and Low Impedances, RSI 10DD.

The current sensitivity of etd (as opposed to voltage sensitivity) is illustrated by Figure 24, which shows etd as a function of epy for high and low ib at two typical operating pressures. In the low impedance case, etd increases with increasing epy (and ib), but in the high impedance case, etd decreases with increasing epy. The conclusion is that an optimum ib exists for minimum etd, and this optimum ib lies somewhere between about 20 and 70 A for the values of interest of P.

For the RSI application, the normal ib is of the order of 20 A. To maintain Bq at a reasonable level, and to ensure that the RSI can withstand the anticipated epy, the column length and geometry are variable only to a limited extent. An important consideration is thus the ratio of etd to epy, which serves as a measure of the effectiveness of the RSI as a closed switch. Figure 25 shows this ratio for the RSI 10DD for both the high and the low current cases, with the tube drop averaged over the pressure values of interest. The increase in etd at high currents is reflected in the curve of Figure 25 which corresponds to the high current case, but in the low current case (which applies for RSI "normal" operation), etd is still in the current region where increases in ib reduce etd. Hence etd/epy continues to decrease materially with increasing epy. The overall conclusion from Figure 25 is that tube drops of only a few percent are indeed feasible for an RSI which operates at high epy with a low Bq.

f. Restrike Phenomenon

Various observations pertaining to the restrike phenomenon have been made during this reporting period but serious efforts to address the matter have yet to be made. It has been found that a significant (if not dominant) fraction of the restrike activity previously reported for RSI's is in fact not true restrike but rather retriggering of the tube caused by ground loop-generated triggering signals and also by spurious noise arising through various mechanisms which are external to the RSI.

Such true restriking as occurs does so in at least two modes. Significant current (1 A) is believed to flow out of the holdoff section through the grid and the triggering circuitry, and this current is certainly sufficient to

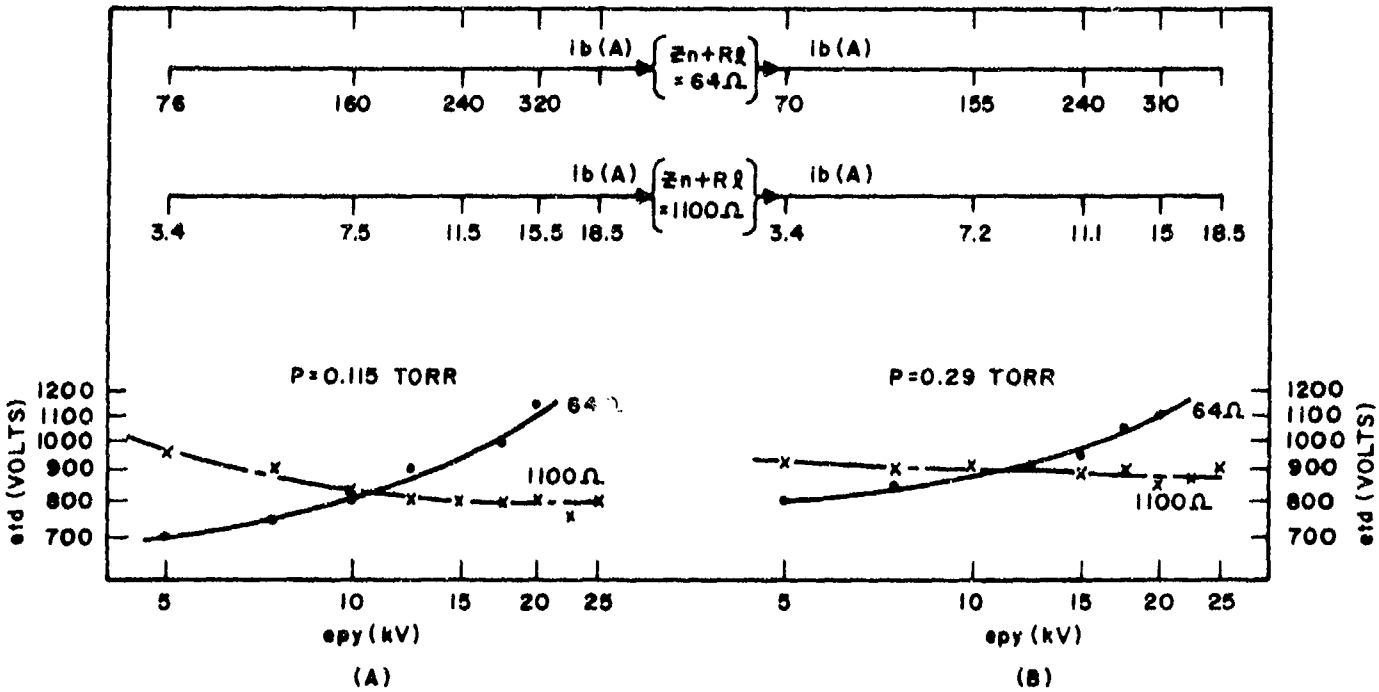

Figure 24. Tube Drop versus epy at Various Tube Pressures and Impedances, RSI 10DD.

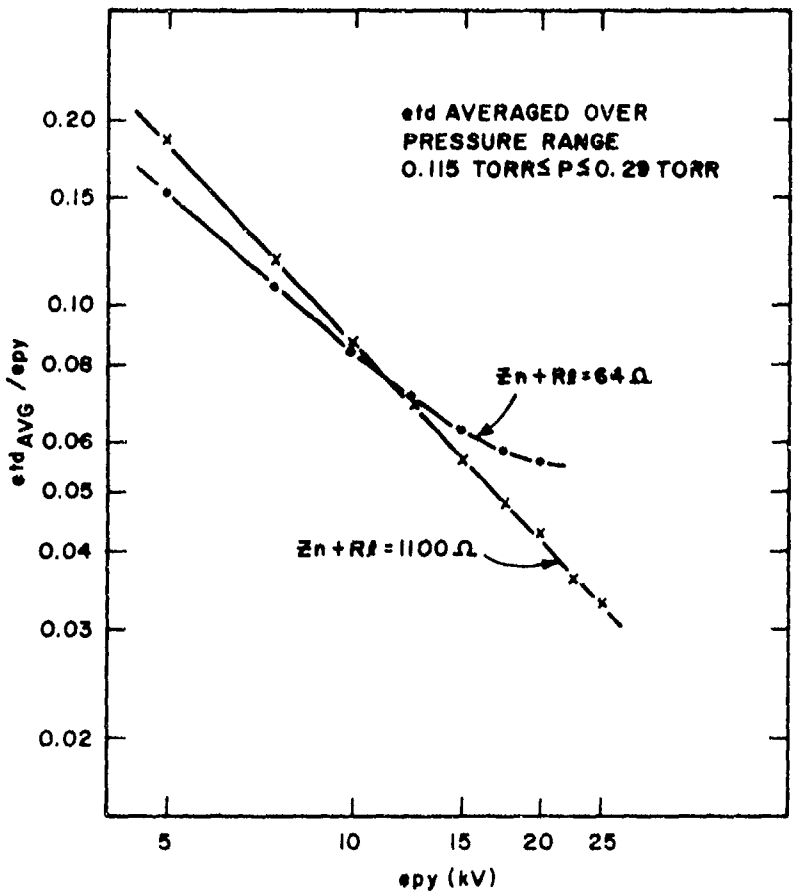

Figure 25. Ratio of Average Total Tube Drop to Peak Forward Anode Voltage, RSI 10DD.

maintain a discharge in the grid-anode region and thus cause restriking of a discharge in the interaction column upon the termination of the pulsed magnetic field. Efforts to reduce this current flow have reduced the incidence of restriking, as have efforts to speed the return of the grid potential to ground prior to the end of the field pulse. None of these brief investigations has been completed because of the more important need to establish the interruption characteristics of the RSI 10 series tubes, and also because the influence of the existing ground loops precludes the detailed waveform analyses which are required to study restrike effectively. It was therefore decided to rebuild the experimental apparatus to eliminate the ground loops subsequent to the characterization of the 10 series tubes. This characterization is now complete.

4.0 CONCLUSIONS AND PLAN FOR FUTURE WORK

a. Conclusions Drawn from the Testing of the RSI 10 Series

The RSI 10 series have proven to be an efficient and reliable family of RSI's which operated successfully at their design voltages and which firmly established the validity of the plasma chute concept as a mechanism for reducing magnetic field requirements without introducing excessively high tube drops. The details of the interruption characteristics for these tubes are somewhat complex but the data have been highly repeatable and no catastrophic tube failures have occurred. Six-hundred ampere interruptions were routinely achieved at 20 kV using the RSI 10DD with an interrupting magnetic field of less than 6 kG peak (magnetic field energy less than 8 joules). Improving the rise time of the magnetic field reduced the need for high peak fields and shows promise as a means for further reducing the overall energy requirements of the magnetic system.

Typical interaction column drops are 400 volts or less per section (corresponding to 26 volts/cm) at reasonable tube pressures with no more than three and possibly two sections being adequate for 50 kV operation. Holdoff section drops of about 120 volts have been observed for sections capable of withstanding 30 kV and which were specifically designed for minimum drop at tube pressures which are consistent with reasonable triggering characteristics and also help to reduce Bq.

The use of multiple, folded interaction sections with the RSI 10DD has been shown not only to provide reliable high voltage interruption, but also to materially reduce Bq. It has also been shown that the presence of a smooth wall behind the discharge tends to reduce Bq, possibly by precluding the existence of a reservoir for plasma which might sustain the discharge.

The restrike situation, although not resolved, appears at least to be amenable to resolution, and such work as has been performed in this area has produced encouraging results.

b. Objectives and Outline of Future Work

The main thrust of Part II of the RSI program is to conduct the research and development necessary to construct five exploratory development RSI's designed to satisfy the operating conditions shown in Table 1, and then to

build and deliver these tubes to ERADCOM. It is clear that every activity pursued under the auspices of the Program should directly enhance the probability for its success, the emphasis being not on research but rather on development. Based on these considerations, a plan for future work has been developed which has positive but limited objectives, and which is consistent with both the remaining time and the current level of funding.

Work will be centered around the RSI 12 series — the five 50 kV tubes actually to be delivered. The long lead times associated with the ceramic interaction sections, and the further assembly time required after their delivery, mandate that the sections be ordered now if the testing of the RSI 12 series tubes is to be completed in a timely fashion. Subsequent to ordering the sections but before their arrival, 50 kV holdoff sections will be designed and fabricated, as will the required cathode and reservoir assemblies. More importantly, the existing RSI 10 series will be used as vehicles to study the restrike phenomenon and also to establish RSI triggering characteristics. Subsequent to testing the RSI 12 series (or possibly concurrent therewith), long duration tests are planned (probably at elevated pulse repetition rates) to determine or at least set a lower bound for RSI service life.

c. RSI 12 Series

Figure 26 shows the interaction channel geometries chosen for the RSI 12 series. The chosen designs represent a careful compromise between the optimum performers of the RSI 10 series (or their logical extensions) and the practical concern of what structures can in fact be fabricated from high alumina ceramic at reasonable cost.

Referring again to Figure 20 where a comparison is made of the various RSI 10 series tubes, one would select Type DD as being the best performer. But the DD was a folded, double-length Type D, and the performance of the D is significantly inferior to that of Types B and E. Next to the DD, and upon examination of the appropriate characteristic curves for Types B and E, one would choose Type E. It is logical that the performance of an "RSI 10EE"

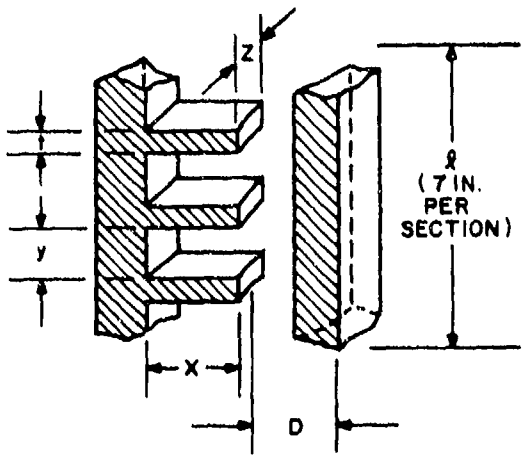

Type	D	x	y	z	Notes
A	0.150	0.250	0.150	0.300	Base Tube
B	0.100	0.250	0.150	0.300	Small Diameter
C	0.150	0.150	0.150	0.300	"End Wall"
D	0.150	0.250	0.100	0.300	Maximum Chutes
E	0.150	0.250	0.125	0.300	Chutes at 45°
F	0.150	0.250	0.150	0.150	Minimum Reservoir

- All dimensions in inches.
- All sections 7 inches long (1).
- Three sections per tube (31).

Figure 26. Schematic Representation of Interaction Channel Geometry, RSI 12 Series.

would have surpassed that of the RSI 1000. Because of the need for reliable operation at 50 kV, and also because a single folding of the D proved so successful, one would choose a hypothetical "RSI-EEE" as the base for a family of 50 kV RSI's, and the various channels of Figure 26 are so based.

A chute wall thickness of 0.075 inch (dimension "t" in Figure 26) is the minimum consistent with ease and safety of fabrication, and this thickness has been chosen to achieve the maximum number of chutes over the length per section, l, which has been set at seven inches to allow sufficient room for insulation at 50 kV with respect to the six-inch-high magnet core. An outer wall thickness of 0.250 inch has been chosen to provide 50 kV insulation to ground through the ceramic at the elevated temperatures corresponding to regular RSI operation.

Six geometries are indicated in the table of Figure 26. Type A is the base. (It is to be understood that each type is a triple section, i.e., Type A is in fact a Type "AAA".) The principal dimensions of interest for each tube type are D, the diameter of the bore; x, the depth of the chute; y, the height of the chute; and z, the width of the chute. The table of Figure 26 summarizes these dimensions, and the more important points are called out here.

All tubes except the B have a bore diameter of 0.150 inch; this diameter worked well with the RSI 10E, the forerunner of this series, as well as with other 10 series tubes. Type B has a bore of 0.100 inch, since in general smaller bores lower Bq. This observation was supported by the data for the 10 series tubes. A bore of 0.100 inch is still safely above the self-quenching current density limit for the RSI "normal" current of 17A.

All tubes except the C have a chute depth of 0.250 inch, which corresponds to the "short" chutes of the 10 series. The purpose of the 0.150 inch chute depth in the C is to determine if the "end wall" aids in interruption.

All tubes except Types D and E have a chute height of 0.150 inch. This is the same height as in the RSI 10E and other 10 series tubes. The purpose of the 0.100 inch chute height in the D is to determine if increasing the number of chutes reduces Bq.

Type 12E is a special case obviously chosen to determine if altering the channel geometry to accommodate the assumed trajectory of the electrons will reduce Bq.

All tubes except the F have a chute width of 0.300 inch, the same width as in the 10 series tubes. The purpose of the 0.150 inch chute width in the F is to determine if minimizing the possible plasma reservoirs will lower Bq.

It is thus clear that the approach used in the design of the RSI 12 series tubes is conservative in that "safe" dimensions have been used throughout, i.e., all "base" dimensions are known to have worked satisfactorily in the past, and in those cases where dimensions have been changed, the change has been in a direction believed to reduce Bq.

d. Restrike

To study restrike effectively, it is necessary to rework the experimental apparatus to eliminate the possibility of ground-loop-generated triggering signals. It is advantageous to do this work now since the 10 series tubes have been characterized, and the 12 series is in the design phase. In addition, the testing of the 12 series requires operation at epy = 50 kV, and the existing apparatus is deemed neither suitable nor safe for operation at this voltage. Operation at 50 kV also requires shielding against X-rays to ensure operator safety, and this work will be done as the apparatus is reworked.

Insofar as the actual restrike investigation is concerned, the voltage waveform at the RSI's grid requires detailed study, as do the anode and grid current waveforms just after interruption. It is mandatory that the grid return to a potential near ground as the holdoff section attempts to recover, or restrike is inevitable. It is also required that the grid circuit be such that no paths exist for a holding current in the holdoff section through the grid circuit. Otherwise the holdoff section can remain in the conducting state, and the discharge in the interaction column can restrike upon the decrease of the magnetic field to some critical value. It may be necessary to specifically tailor the pulse shape at the grid or to shape the field pulse to investigate these effects, but the ultimate goal is the elimination of restrike as opposed to its accommodation.

e. Trigger Characterization and Life Testing

It is feasible but not particularly desirable to operate an RSI in a perpetually triggered mode such that each conduction period requires the application of a pulse to the grid of the device. The work reported here was performed with the RSI operated in this fashion.

It is more advantageous to maintain the RSI in a free-running mode via a "keep-alive" current such that the only pulse applied to the device is the magnetic field necessary to interrupt the discharge. Investigations are required to determine the required amount of keep-alive power and the most suitable mode (DC or pulsed) for its application. The effects of keep-alive on restrike will also be determined.

Long duration life testing is also required to determine the most probable failure mechanism for RSI tubes, and such testing is best performed at relatively high (at least 1 kHz) pulse repetition rates. The effects on Bq and restrike of such residual ionization as may exist at high pulse rates is as yet unknown, as are the effects of electrode and interaction column heating due to operation at high average and RMS currents. Triggering studies and life testing at high pulse repetition rates are therefore planned to gain insight as to the overall performance characteristics of practical RSI's.

5.0 REFERENCES AND BIBLIOGRAPHY

1. Simon, R., and Turnquist, D.V., "Repetitive Series Interrupter II," Research and Development Technical Report ECOM-76-1301-3, May 1977.

2. Simon, R., and Turnquist, D.V., "Repetitive Series Interrupter II," Research and Development Technical Report ECOM-76-1301-4, July 1977.

3. Simon, R., and Turnquist, D.V., "Repetitive Series Interrupter II," Research and Development Technical Report ECOM-76-1301-5, January 1978.

4. Simon, R., and Turnquist, D.V., "Repetitive Series Interrupter II," Research and Development Technical Report ECOM-76-1301-F, April 1978.

The above documents in conjunction with two earlier technical reports (ECOM-76-1301-1 and -2 dated December 1976 and March 1977, respectively) discuss the results of Part I of the RSI Program.

For earlier work on magnetically controlled gas discharge switches, see:

Turnquist, D.V., "Magnetic Field Control of a Gas Discharge Switch," Proc. 9th Modulator Symposium, U.S. Army Electronics Command, May 1966.

Thomas, J., Vandenbrink, H., and Turnquist, D.V., "New Switching Concepts," Technical Report ECOM 00123-F, October 1967.

Shackleford, C., "Repetitive Series Interrupter," Technical Report ECOM-73-0320-F, September 1974.

Weldon, R.J. "A Thyratron with Magnetic Interruption," Proc. IEEE 12th Modulator Symposium, 1976.

Weiner, M., "Repetitive Series Interrupter," IEEE 12th Modulator Symposium, 1976.

DISTRIBUTION LIST

12 Defense Documentation Center
ATTN: DDC-TCA
Cameron Station (Bldg 5)
Alexandria, VA 22314

1 Code R123, Tech Library
DCA Defense Comm Engrg Ctr
1860 Wiehle Ave
Reston, VA 22090

1 Defense Communications Agency
Technical Library Center
Code 205 (P. A. TOLOVI)
Washington, DC 20305

1 Office of Naval Research
Code 427
Arlington, VA 22217

1 Director
Naval Research Laboratory
ATTN: Code 2627
Washington, DC 20375

1 Commander
Naval Electronics Laboratory Center
ATTN: Library
San Diego, CA 92152

1 CDR, Naval Surface Weapons Center
White Oak Laboratory
ATTN: Library, Code WX-21
Silver Spring, MD 20910

1 Rome Air Development Center
ATTN: Documents Library (TILD)
Griffiss AFB, NY 13441

1 Hq, Air Force Systems Command
ATTN: DLCA
Andrews AFB
Washington, DC 20331

2 CDR, US Army Missile Command
Redstone Scientific Info Center
ATTN: Chief, Document Section
Redstone Arsenal, AL 35809

1 Commander
US Army Missile Command
ATTN: DRSMI-RE (Mr. Pittman)
Redstone Arsenal, AL 35809

3 Commandant
US Army Aviation Center
ATTN: ATZQ-D-MA
Fort Rucker, AL 36362

1 Director, Ballistic Missile Defense
Advanced Technology Center
ATTN: ATC-R, PO BOX 1500
Huntsville, AL 35807

1 Commander
HQ Fort Huachuca
ATTN: Technical Reference Div
Fort Huachuca, AZ 85613

2 Commander
US Army Electronic Proving Ground
ATTN: STEEP-MT
Fort Huachuca, AZ 85613

1 Commander
USASA Test & Evaluation Center
ATTN: IAO-CDR-T
Fort Huachuca, AZ 85613

1 Deputy for Science & Technology
Office, Assist Sec Army (R&D)
Washington, DC 20310

1 CDR, Harry Diamond Laboratories
ATTN: Library
2800 Powder Mill Road
Adelphi, MD 20783

1 Director
US Army Ballistic Research Labs
ATTN: DRXBR-LB
Aberdeen Proving Ground, MD 21005

1 Harry Diamond Laboratories, Dept of Army
ATTN: DRXDO-RCB (Dr. J. Nemarich)
2800 Powder Mill Road
Adelphi, MD 20783

1 Commander
US Army Tank-Automotive Command
ATTN: DRDTA-RH
Warren, MI 48090

1 CDR, US Army Aviation Systems Command
ATTN: DRSAV-G
PO Box 209
St. Louis, MO 63166

1 TRI-TAC Office
ATTN: CSS (Dr. Pritchard)
Fort Monmouth, NJ 07703

1 CDR, US Army Research Office
ATTN: DRXRO-IP
PO Box 12211
Research Triangle Park, NC 27709

1 CDR, US Army Research Office
ATTN: DRXRO-PH (Dr. R. J. Lontz)
PO Box 12211
Research Triangle Park, NC 27709

1 Commandant
US Army Air Defense School
ATTN: ATSA-CD-MC
Fort Bliss, TX 79916

1 Commander, DARCOM
ATTN: DRCDE
5001 Eisenhower Ave
Alexandria, VA 22333

1 Naval Surface Weapons Center
Dahlgren Laboratory
ATTN: Dr. M. Rose, Code DF-102
Dahlgren, VA 22448

1 Ballistic Missile Defense Advanced Technology Center
ATTN: Dr. L. Havard, ATC-T
P.O. Box 1500
Huntsville, AL 35807

1 Air Force Aero Propulsion Laboratory
ATTN: Mr. R. Verga, AFAPL/POD-1
Wright Patterson Air Force Base
Ohio 45433

1 Chief
Ofc of Missile Electronic Warfare
Electronic Warfare Lab, ECOM
White Sands Missile Range, NM 88002

Commander
US Army Electronics Command
Fort Monmouth, NJ 07703
1 DRSEL-GG-TD
1 DRSEL-WL-D
3 DRSEL-CT-D
1 DRSEL-TL-DT
3 DRSEL-TL-BG
1 DRSEL-TL-BG (Ofc of Record)
2 DRSEL-MS-TI
1 DRSEL-TL-D
25 Originating Office

2 MIT - Lincoln Laboratory
ATTN: Library (RM A-082)
PO Box 73
Lexington, MA 02173

1 NASA Scientific & Tech Info Facility
Baltimore/Washington Intl Airport
PO Box 8757, MD 21240

2 Advisory Group on Electron Devices
201 Varick Street, 9th Floor
New York, NY 10014

1 ITT Electron Tube Division
3100 Charlotte Avenue
Easton, PA 18042